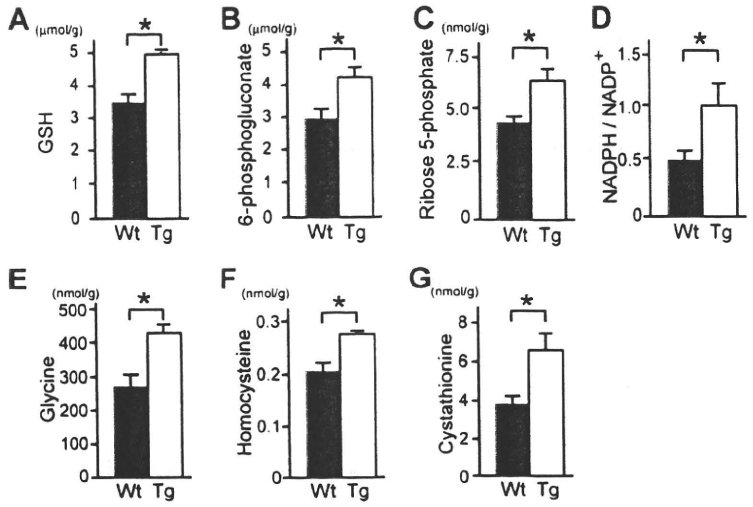

Figure 6. Metabolome analysis of *Aldh2*2* Tg hearts. A, Intracellular reduced GSH levels were measured using BIOXYTECH GSH/GSSG-412 based on Tietze methods. B through G, 6-Phosphogluconate, ribose-5-phosphate, NADPH/NADP$^+$ ratio, glycine, homocysteine, and cystathionine levels measured by CE-MS. Data are the means±SEM (n=6 to 8). $^*P<0.05$ (unpaired Student's *t* test).

hearts and attenuated the oxidative stress–resistant phenotype. These findings indicate that Atf4-dependent activation of amino acid metabolism and GSH biosynthesis are causally involved in the oxidative stress–resistant phenotype observed in mitochondrial Aldh–deficient hearts. Enhanced supply of NADPH via the pentose phosphate pathway concomitantly helps in the recycling of oxidized GSH (GSH disulfide [GSSG]).

Here, we showed that the forced expression of Aldh2*2 in the heart impairs Aldh activity against aliphatic aldehydes, including 4-HNE. Several lines of evidence suggest that ALDH2*2 inactivates not only ALDH2 but also other ALDH subfamilies by forming heterotetramers.[22,23] For example, alignment of ALDH2 and ALDH1B1 amino acid sequences reveals a high degree of conservation between the regions required for dimer formation (ie, the α-helix G residues 247 to 259, β-sheet 18 residues 450 to 453, β-sheet 19 residues 486 to 495, and the "oligomerization domain" residues 140 to 158 and 486 to 495). Notably, there is 100% conservation of residues involved in tetramer formation (ie, β-sheet 5 residues 141 to 144). These findings suggest that ALDH1B1 is one of the targets of ALDH2*2. We are currently investigating other enzymes that are inactivated by Aldh2*2.

However, kinetic assays may not address overall metabolic function or changes in other metabolic pathways, and increases in Gsta1/2 levels seen in the *Aldh2*2* Tg hearts may compensate for defects in mitochondrial Aldh activity. A cell fractionation study revealed Aldh2*2 protein in the mitochondria. Consistent with this, we found that some 4-HNE adduct proteins were also increased in the mitochondrial fraction of *Aldh2*2* Tg hearts. Furthermore, 4-HNE immunoreactivity was increased following adenovirus-mediated

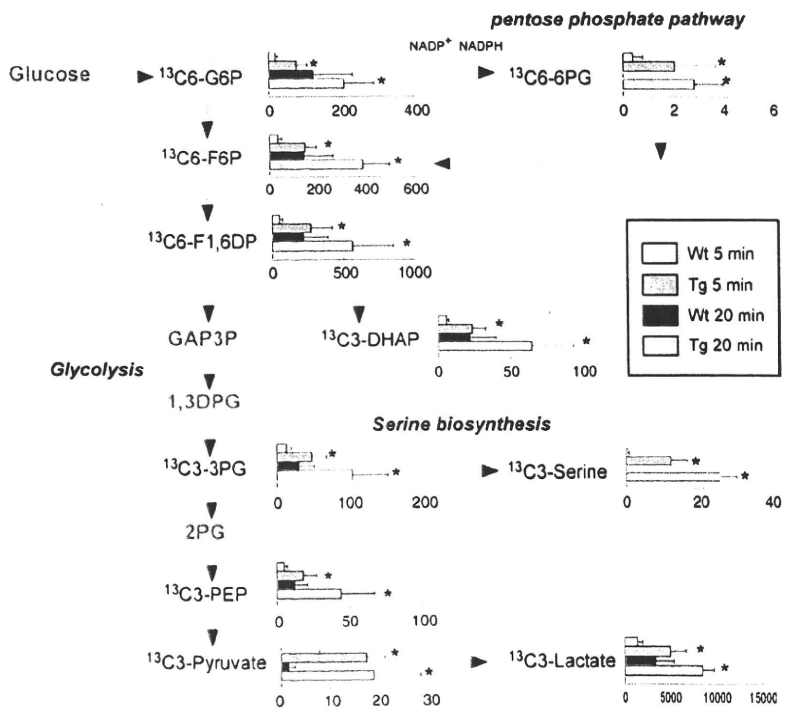

Figure 7. Fluxome analysis of *Aldh2*2* Tg hearts. Isolated hearts from Wt and *Aldh2*2* Tg mice were perfused with modified Krebs–Henseleit buffer containing 10 mmol/L ^{13}C-glucose, 10 μU/mL insulin, 0.4 mmol/L oleate, and 1% BSA. ^{13}C-Labeled metabolites were quantified by CE-MS after 5 and 20 minutes. Note that ^{13}C-serine biosynthesis was increased in *Aldh2*2* Tg hearts. Data are the means±SEM (n=6). $^*P<0.05$ vs Wt control (unpaired Student's *t* test). G6P indicates glucose 6-phosphate; F6P, fructose 6-phosphate; F1,6DP, fructose 1,6-bisphosphate; GAP3P, glyceraldehyde 3-phosphate; DHAP, dihydroxyacetone phosphate; 1,3DPG, 1,3-bisphosphoglycerate; 3PG, 3-phosphoglycerate; 2PG, 2-phosphoglycerate; PEP, phosphoenolpyruvate; 6PG, 6-phosphogluconate.

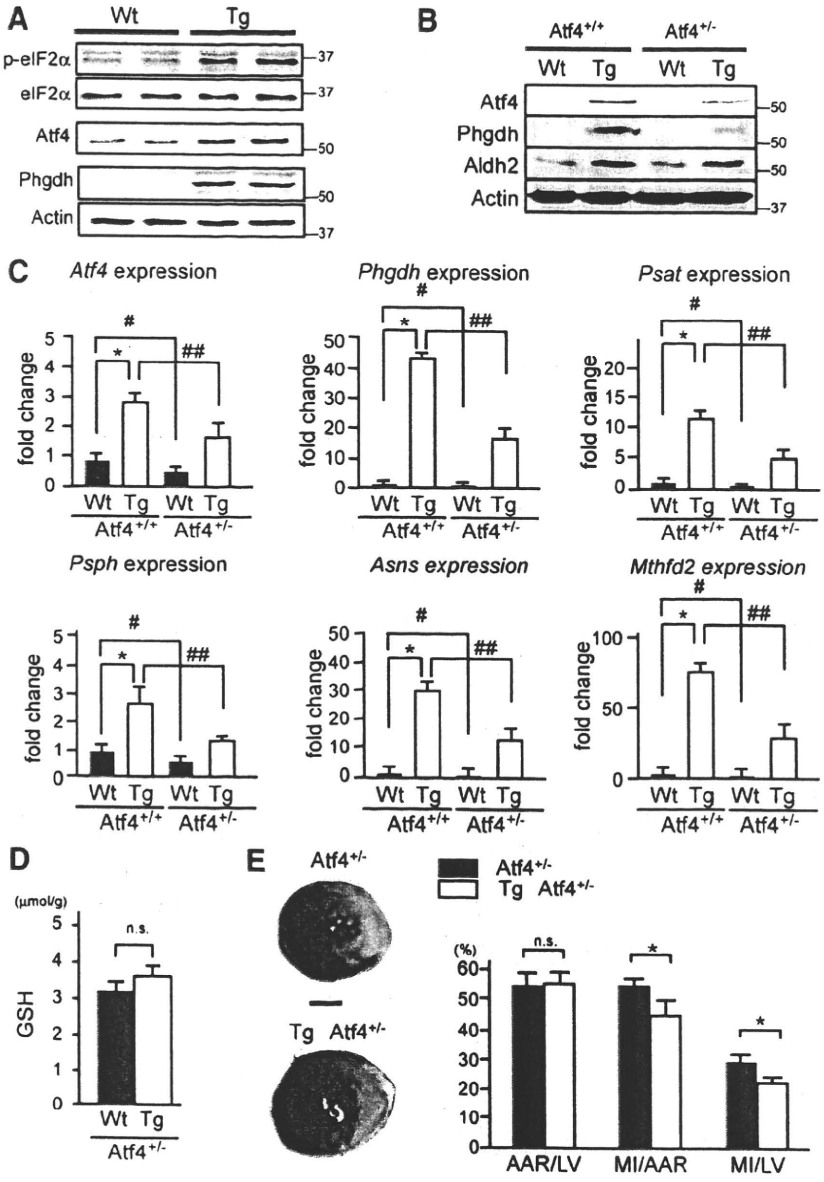

Figure 8. Role of Atf4 in the oxidative stress–resistant phenotype of *Aldh2*2* Tg hearts. A, Comparisons of eIF2α phosphorylation and protein expression of Atf4 and Phgdh between hearts from *Aldh2*2* Tg mice and their Wt littermates. B and D, Effects of heterogeneous Atf4 knockout on protein expression of Atf4 and Phgdh (B) and GSH levels (D) in hearts from *Aldh2*2* Tg and Wt mice. C and E, Heterogeneous Atf4 knockout suppressed the induction of genes for enzymes involved in amino acid metabolism (C) and the oxidative stress–resistant phenotype observed for *Aldh2*2* Tg hearts (E). E (left), Representative images of hearts from *Aldh2*2* Tg and Wt mice against the *Atf4* $^{-/-}$ background (*Atf4* $^{-/-}$) after I/R injury. Bar=2 mm. Right, Quantification of infarct size. AAR indicates area at risk; LV, total left ventricular area; MI, area of myocardial infarction. Data are the means±SEM (n=8). **P*<0.05; #*P*<0.05; ##*P*<0.05.

overexpression of Aldh2*2 in cultured cardiomyocytes. Together, these results strongly suggested that aldehyde metabolism in mitochondria is indeed affected in the Tg hearts.

Myocardial GSH content influences susceptibility to I/R injury.[30] The rate of GSH synthesis is determined primarily by γ-glutamyl-cysteine ligase activity and the availability of precursor amino acids, especially cysteine. In the present study, there was only marginal induction of the GSH biosynthetic enzyme γ-glutamyl-cysteine ligase in *Aldh2*2* Tg hearts. In contrast, significant upregulation was observed in *Aldh2*2* Tg hearts of genes encoding enzymes involved in serine biosynthesis (*Phgdh*, *Psat1*, and *Psph*), the conversion of serine to glycine (*Shmt1/2*), the *trans*-sulfuration pathway (*Cth*), and the transportation of cysteine and cystine (*Slc1A4*, *Slc3A2*).[31] Because γ-glutamyl-cysteine ligase activity is subject to feedback inhibition by increased levels of GSH,[32] we speculate that activation of the biosynthesis and transport of precursor amino acids plays a key role in the maintenance of higher levels of GSH biosynthesis for cardioprotection.

Using fluxome analysis, we confirmed the increased flux toward the glycolytic and pentose phosphate pathways in *Aldh2*2* Tg hearts. Enhanced flux toward the pentose phosphate pathway should be linked with the amount of $NADP^+$ provided by GSH reductase, which converts GSSG to GSH. Because the NADPH/$NADP^+$ ratio is increased in *Aldh2*2* Tg hearts, there may be an active mechanism to shift glucose biotransformation from glycolysis toward the pentose phosphate pathway. The precise mechanism underlying the redirection of metabolic flux from the glycolytic to the pentose phosphate pathway under conditions of oxidative stress remains unknown.[33,34]

The present work has extended the concept of cardioprotection by preconditioning. According to the present understanding of cardioprotection by preconditioning,[35] mitochondria are targets for protection from cell death. During sustained ischemia and reperfusion, the opening of the mitochondrial permeability transition pore induces mitochon-

drial swelling, depolarization, and ultimately cell death. Cardioprotection by preconditioning induced by brief nonlethal episodes of I/R activates a variety of signaling cascades, all of which culminate in the inhibition of mitochondrial permeability transition pore opening. Here, we showed that mitochondrial retrograde signals (signals originating from mitochondria)[36] play a key role in cardioprotection. A shift toward the oxidative state in mitochondrial matrices signals to the nucleus to change nuclear gene expression, enabling cells to adapt and thus compensate for mitochondrial oxidative stress. Moreover, these signals favor tolerance to acute I/R injury. We also demonstrated that the eIF2α-Atf4 pathway provides the key mitochondrial retrograde signals in response to mitochondrial aldehyde stress. Interestingly, characteristic transcriptional changes in *Aldh2**2 Tg hearts were observed in human hybrid cells that harbor MELAS (mitochondrial myopathy, encephalopathy, lactic acidosis, stroke-like episode) and NARP (neurogenic muscle weakness, ataxia, and retinitis pigmentosa) mitochondrial DNA mutations[37] and in frataxin-deficient murine hearts (Friedreich's ataxia model),[38] which are characterized by mitochondrial dysfunction and oxidative stress.

This study was limited by the uncertainty as to whether the cardioprotection observed for the *Aldh2**2 Tg hearts actually exists in individuals carrying the *ALDH2**2 allele. More generally, it would be intriguing to know whether a mitochondrial retrograde response transduced via the eIF2α-ATF4 pathway is involved in cardioprotection during human aging and age-related diseases. Aging is accompanied by increased reactive oxygen species production and increased oxidative damage to mitochondrial DNA, proteins, and lipids.[39] In addition, loss of cardioprotection in aged hearts[40] is a likely consequence of the age-associated reduction in retrograde-response signaling. Notably, a paradoxical decline in the relative levels of eIF2α phosphorylation and ATF4 expression were demonstrated in aged rat tissues including heart,[41] suggesting that the eIF2α-ATF4-mediated retrograde response to mitochondrial dysfunction would also operate less efficiently in aged heart. How this retrograde regulation is affected by aging and age-related diseases represents an important area of future research.

The present study provides insight into the clinical significance of the hormesis-like effects of aldehydes. Hormesis is generally defined as a biphasic dose–response curve to treatments that are beneficial at low levels but noxious at higher levels.[42] However, for practical reasons, most researchers in the fields of aging and molecular biology use a limited number of doses in the optimal or hormetic zone to study adaptive mechanisms. Thus, these researchers report hormetic effects without having to confirm a biphasic dose–response curve. This is certainly true for many examples of preconditioning.[43,44] We extend the concept to hormetic mimetics: the fact that exposure occurs throughout life is not a problem, because the hormetic effects can be induced within the setting of chronic exposure that persists throughout the lifetime of mice.

Mitochondrial aldehyde stress produces different tissue-specific outcomes. It is essential to determine how aldehydes switch between being a hormetic signal and cytotoxicity and any alternative functions of aldehydes. Given the central role of aldehydes in the stress-induced signaling required to establish hormetic conditions, mimetic triggers of hormesis may be a promising approach for the prevention of the onset of age-associated diseases and senescence itself without the risk of overwhelming damage associated with the use of aldehydes themselves.

Acknowledgments

We thank M. Nishijima, EJ. Calabrese, Y. Oike, N. Mizushima, and Y. Suzuki for critical discussions and K. Kaneki, M. Abe, M. Doi, Y. Miyake, and Y. Shiozawa for technical assistance. M. Sano, T.A., and M. Suematsu are core members of the Global Center of Excellence (GCOE) for Human Metabolomics Systems Biology, Ministry of Education, Culture, Sports, Science and Technology.

Sources of Funding

This work was supported by a PRESTO (Metabolism and Cellular Function) grant from the Japanese Science and Technology Agency (to M. Sano) and also by NIH grants EY11490 and EY AA016875 (to V.V.).

Disclosures

None.

References

1. Conklin D, Prough R, Bhatanagar A. Aldehyde metabolism in the cardiovascular system. *Mol Biosyst.* 2007;3:136–150.
2. Watson AD, Leitinger N, Navab M, Faull KF, Horkko S, Witztum JL, Palinski W, Schwenke D, Salomon RG, Sha W, Subbanagounder G, Fogelman AM, Berliner JA. Structural identification by mass spectrometry of oxidized phospholipids in minimally oxidized low density lipoprotein that induce monocyte/endothelial interactions and evidence for their presence in vivo. *J Biol Chem.* 1997;272:13597–13607.
3. Veronneau M, Comte B, Des Rosiers C. Quantitative gas chromatographic-mass spectrometric assay of 4-hydroxynonenal bound to thiol proteins in ischemic/reperfused rat hearts. *Free Radic Biol Med.* 2002;33:1380–1388.
4. Liu Q, Raina AK, Smith MA, Sayre LM, Perry G. Hydroxynonenal, toxic carbonyls, and Alzheimer disease. *Mol Aspects Med.* 2003;24:305–313.
5. Dickinson DA, Iles KE, Watanabe N, Iwamoto T, Zhang H, Krzywanski DM, Forman HJ. 4-hydroxynonenal induces glutamate cysteine ligase through JNK in HBE1 cells. *Free Radic Biol Med.* 2002;33:974.
6. Uchida K, Shiraishi M, Naito Y, Torii Y, Nakamura Y, Osawa T. Activation of stress signaling pathways by the end product of lipid peroxidation. 4-hydroxy-2-nonenal is a potential inducer of intracellular peroxide production. *J Biol Chem.* 1999;274:2234–2242.
7. Yang Y, Sharma R, Sharma A, Awasthi S, Awasthi YC. Lipid peroxidation and cell cycle signaling: 4-hydroxynonenal, a key molecule in stress mediated signaling. *Acta Biochim Pol.* 2003;50:319–336.
8. Vasiliou V, Pappa A, Estey T. Role of human aldehyde dehydrogenases in endobiotic and xenobiotic metabolism. *Drug Metab Rev.* 2004;36:279–299.
9. Vasiliou V, Nebert DW. Analysis and update of the human aldehyde dehydrogenase (ALDH) gene family. *Hum Genomics.* 2005;2:138–143.
10. Ohsawa I, Nishimaki K, Yasuda C, Kamino K, Ohta S. Deficiency in a mitochondrial aldehyde dehydrogenase increases vulnerability to oxidative stress in PC12 cells. *J Neurochem.* 2003;84:1110–1117.
11. Ohta S, Ohsawa I, Kamino K, Ando F, Shimokata H. Mitochondrial ALDH2 deficiency as an oxidative stress. *Ann N Y Acad Sci.* 2004;1011:36–44.
12. Gaziano JM, Gaziano TA, Glynn RJ, Sesso HD, Ajani UA, Stampfer MJ, Manson JE, Hennekens CH, Buring JE. Light-to-moderate alcohol consumption and mortality in the Physicians' Health Study enrollment cohort. *J Am Coll Cardiol.* 2000;35:96–105.
13. Krenz M, Baines CP, Yang XM, Heusch G, Cohen MV, Downey JM. Acute ethanol exposure fails to elicit preconditioning-like protection in in situ rabbit hearts because of its continued presence during ischemia. *J Am Coll Cardiol.* 2001;37:601–607.

14. Churchill EN, Disatnik MH, Mochly-Rosen D. Time-dependent and ethanol-induced cardiac protection from ischemia mediated by mitochondrial translocation of varepsilonPKC and activation of aldehyde dehydrogenase 2. *J Mol Cell Cardiol*. 2009;46:278–284.
15. Chen CH, Budas GR, Churchill EN, Disatnik MH, Hurley TD, Mochly-Rosen D. Activation of aldehyde dehydrogenase-2 reduces ischemic damage to the heart. *Science*. 2008;321:1493–1495.
16. Larson HN, Zhou J, Chen Z, Stamler JS, Weiner H, Hurley TD. Structural and functional consequences of coenzyme binding to the inactive Asian variant of mitochondrial aldehyde dehydrogenase: roles of residues 475 and 487. *J Biol Chem*. 2007;282:12940–12950.
17. Enomoto N, Takase S, Yasuhara M, Takada A. Acetaldehyde metabolism in different aldehyde dehydrogenase-2 genotypes. *Alcohol Clin Exp Res*. 1991;15:141–144.
18. Ohsawa I, Kamino K, Nagasaka K, Ando F, Niino N, Shimokata H, Ohta S. Genetic deficiency of a mitochondrial aldehyde dehydrogenase increases serum lipid peroxides in community-dwelling females. *J Hum Genet*. 2003;48:404–409.
19. Kamino K, Nagasaka K, Imagawa M, Yamamoto H, Yoneda H, Ueki A, Kitamura S, Namekata K, Miki T, Ohta S. Deficiency in mitochondrial aldehyde dehydrogenase increases the risk for late-onset Alzheimer's disease in the Japanese population. *Biochem Biophys Res Commun*. 2000;273:192–196.
20. Ohsawa I, Nishimaki K, Murakami Y, Suzuki Y, Ishikawa M, Ohta S. Age-dependent neurodegeneration accompanying memory loss in transgenic mice defective in mitochondrial aldehyde dehydrogenase 2 activity. *J Neurosci*. 2008;28:6239–6249.
21. Isse T, Oyama T, Kitagawa K, Matsuno K, Matsumoto A, Yoshida A, Nakayama K, Nakayama K, Kawamoto T. Diminished alcohol preference in transgenic mice lacking aldehyde dehydrogenase activity. *Pharmacogenetics*. 2002;12:621–626.
22. Steinmetz CG, Xie P, Weiner H, Hurley TD. Structure of mitochondrial aldehyde dehydrogenase: the genetic component of ethanol aversion. *Structure*. 1997;5:701–711.
23. Isse T, Matsuno K, Oyama T, Kitagawa K, Kawamoto T, Aldehyde dehydrogenase 2 gene targeting mouse lacking enzyme activity shows high acetaldehyde level in blood, brain, and liver after ethanol gavages. *Alcohol Clin Exp Res*. 2005;29:1959–1964.
24. Lu SC. Regulation of glutathione synthesis. *Curr Top Cell Regul*. 2000;36:95–116.
25. Wek RC, Jiang HY, Anthony TG. Coping with stress: eIF2 kinases and translational control. *Biochem Soc Trans*. 2006;34(pt 1):7–11.
26. Kilberg MS, Pan YX, Chen H, Leung-Pineda V. Nutritional control of gene expression: how mammalian cells respond to amino acid limitation. *Annu Rev Nutr*. 2005;25:59–85.
27. Rutkowski DT, Kaufman RJ. All roads lead to ATF4. *Dev Cell*. 2003;4:442–444.
28. Harding HP, Zhang Y, Zeng H, Novoa I, Lu PD, Calfon M, Sadri N, Yun C, Popko B, Paules R, Stojdl DF, Bell JC, Hettmann T, Leiden JM, Ron D. An integrated stress response regulates amino acid metabolism and resistance to oxidative stress. *Mol Cell*. 2003;11:619–633.
29. Tanaka T, Tsujimura T, Takeda K, Sugihara A, Maekawa A, Terada N, Yoshida N, Akira S. Targeted disruption of ATF4 discloses its essential role in the formation of eye lens fibres. *Genes Cells*. 1998;3:801–810.
30. Singh A, Lee KJ, Lee CY, Goldfarb RD, Tsan MF. Relation between myocardial glutathione content and extent of ischemia-reperfusion injury. *Circulation*. 1989;80:1795–1804.
31. Lo M, Wang YZ, Gout PW. The x (c) - cystine/glutamate antiporter: a potential target for therapy of cancer and other diseases. *J Cell Physiol*. 2008;215:593–602.
32. Seelig GF, Simondsen RP, Meister A. Reversible dissociation of gamma-glutamylcysteine synthetase into two subunits. *J Biol Chem*. 1984;259:9345–9347.
33. Uchida K, Stadtman ER. Modification of histidine residues in proteins by reaction with 4-hydroxynonenal. *Proc Natl Acad Sci U S A*. 1992;89:4544–4548.
34. Hammes HP, Du X, Edelstein D, Taguchi T, Matsumura T, Ju Q, Lin J, Bierhaus A, Nawroth P, Hannak D, Neumaier M, Bergfeld R, Giardino I, Brownlee M. Benfotiamine blocks three major pathways of hyperglycemic damage and prevents experimental diabetic retinopathy. *Nat Med*. 2003;9:294–299.
35. Heusch G, Boengler K, Schulz R. Cardioprotection: nitric oxide, protein kinases, and mitochondria. *Circulation*. 2008;118:1915–1919.
36. Liu Z, Butow RA. Mitochondrial retrograde signaling. *Annu Rev Genet*. 2006;40:159–185.
37. Fujita Y, Ito M, Nozawa Y, Yoneda M, Oshida Y, Tanaka M. CHOP (C/EBP homologous protein) and ASNS (asparagine synthetase) induction in cybrid cells harboring MELAS and NARP mitochondrial DNA mutations. *Mitochondrion*. 2007;7:80–88.
38. Seznec H, Simon D, Bouton C, Reutenauer L, Hertzog A, Golik P, Procaccio V, Patel M, Drapier JC, Koenig M, Puccio H, Friedreich ataxia: the oxidative stress paradox. *Hum Mol Genet*. 2005;14:463–474.
39. Finley LW, Haigis MC. The coordination of nuclear and mitochondrial communication during aging and calorie restriction. *Ageing Res Rev*. 2009;8:173–188.
40. Boengler K, Schulz R, Heusch G. Loss of cardioprotection with ageing. *Cardiovasc Res*. 2009;83:247–261.
41. Hussain SG, Ramaiah KV. Reduced eIF2alpha phosphorylation and increased proapoptotic proteins in aging. *Biochem Biophys Res Commun*. 2007;355:365–370.
42. Calabrese EJ, Baldwin LA, Holland CD. Hormesis: a highly generalizable and reproducible phenomenon with important implications for risk assessment. *Risk Anal*. 1999;19:261–281.
43. Gems D, Partridge L. Stress-response hormesis and aging: "that which does not kill us makes us stronger." *Cell Metab*. 2008;7:200–203.
44. Sano M, Fukuda K. Activation of mitochondrial biogenesis by hormesis. *Circ Res*. 2008;103:1191–1193.

Nongenetic method for purifying stem cell–derived cardiomyocytes

Fumiyuki Hattori[1,2], Hao Chen[1,3], Hiromi Yamashita[1], Shugo Tohyama[1,3], Yu-suke Satoh[1,4], Shinsuke Yuasa[1], Weizhen Li[1], Hiroyuki Yamakawa[1,3], Tomofumi Tanaka[1,2], Takeshi Onitsuka[1,3], Kenichiro Shimoji[1,3], Yohei Ohno[1,3], Toru Egashira[1,3], Ruri Kaneda[1], Mitsushige Murata[1,3], Kyoko Hidaka[5], Takayuki Morisaki[5], Erika Sasaki[6], Takeshi Suzuki[4], Motoaki Sano[1], Shinji Makino[1], Shinzo Oikawa[2] & Keiichi Fukuda[1]

Several applications of pluripotent stem cell (PSC)-derived cardiomyocytes require elimination of undifferentiated cells. A major limitation for cardiomyocyte purification is the lack of easy and specific cell marking techniques. We found that a fluorescent dye that labels mitochondria, tetramethylrhodamine methyl ester perchlorate, could be used to selectively mark embryonic and neonatal rat cardiomyocytes, as well as mouse, marmoset and human PSC-derived cardiomyocytes, and that the cells could subsequently be enriched (>99% purity) by fluorescence-activated cell sorting. Purified cardiomyocytes transplanted into testes did not induce teratoma formation. Moreover, aggregate formation of PSC-derived cardiomyocytes through homophilic cell-cell adhesion improved their survival in the immunodeficient mouse heart. Our approaches will aid in the future success of using PSC-derived cardiomyocytes for basic and clinical applications.

Human embryonic stem cells (ESCs) and induced pluripotent stem cells (iPSCs) could prove to be an unlimited source of cardiomyocytes. Several studies have achieved directed differentiation of mouse, monkey and human ESCs into cardiomyocytes[1–3] but with variable efficiency. Some protocols describe up to 60% differentiation efficiency, but none achieve >99% of cells differentiating into cardiomyocytes without the use of genetic selection methods[4]. Transplantation of undifferentiated ESCs results in the formation of teratomas[5]. Thus, it is necessary to purify ESC-derived cardiomyocytes before transplantation.

ESC lines with various combinations of cardiomyocyte-specific reporters can be used to obtain highly pure ESC-derived cardiomyocytes[4,6–10], but this requires genetic modification of the cells. Also, discontinuous Percoll density gradient centrifugation could be used to enrich for mouse and human ESC-derived cardiomyocytes, but the purity of the cardiomyocytes in these preparations is relatively low[11,12]. Here we show that cardiomyocytes in early mouse embryos or those differentiated from pluripotent stem cells (PSCs) have high mitochondrial content and can be purified without the need for genetic modification, using fluorescent dyes that label mitochondria.

RESULTS

Characterization of mitochondrial dyes

In primary cultures of neonatal rat heart cells stained with MitoTracker Red (Invitrogen) the fluorescence intensity of cardiomyocytes was much higher compared to that of nonmyocytes (**Fig. 1a**). MitoTracker Red and tetramethylrhodamine methyl ester perchlorate (TMRM) specifically accumulated in both the subsarcomeric mitochondria, located around the nucleus and in the intermyofibrillar mitochondria (**Fig. 1a** and **Supplementary Fig. 1**). To confirm specific mitochondrial staining of MitoTracker dyes, we stained neonatal rat cardiomyocytes with MitoTracker Red and JC-1 (a mitochondrial voltage-sensitive dye; **Supplementary Fig. 2**).

Fluorescence-activated cell sorter (FACS) analysis of cells dissociated from neonatal heart revealed three main populations (**Fig. 1b**). We sorted the populations with the highest (designated as fraction 1), the middle (fraction 2) and the lowest (fraction 3) fluorescence intensity and cultured them separately. All the cells in fraction 1 showed rhythmic beating and were immunostained with an antibody to α-actinin (**Fig. 1c**), indicating they were cardiomyocytes. We identified very few cardiomyocytes in fraction 2 (**Fig. 1c**). Fraction 3 consisted of red blood cells and dead cells. We confirmed the neonatal rat cardiomyocyte content in fraction 1 by immunofluorescence staining for α-actinin to be 99.4 ± 0.6% (**Fig. 1d**), and the yield was approximately 5×10^5 cells from a single heart.

Next, we compared the efficacy of various mitochondrial dyes for separating the neonatal rat cardiomyocyte population from the nonmyocytes and found that TMRM was the most effective (**Fig. 1e,f**). We then evaluated the washout efficiencies of the dyes and found that TMRM disappeared completely within 24 h, whereas

[1]Department of Regenerative Medicine and Advanced Cardiac Therapeutics, Keio University School of Medicine, Tokyo, Japan. [2]Asubio Pharma Co., Ltd., Osaka, Japan. [3]Division of Cardiology, Department of Medicine, Keio University School of Medicine, Tokyo, Japan. [4]Division of Basic Biological Sciences, Faculty of Pharmacy, Keio University, Tokyo, Japan. [5]Department of Bioscience, National Cardiovascular Center Research Institute, Osaka, Japan. [6]Laboratory of Applied Developmental Biology, Marmoset Research Department, Central Institute for Experimental Animals, Kanagawa, Japan. Correspondence should be addressed to K.F. (kfukuda@sc.itc.keio.ac.jp).

RECEIVED 10 AUGUST; ACCEPTED 15 OCTOBER; PUBLISHED ONLINE 29 NOVEMBER 2009; DOI:10.1038/NMETH.1403

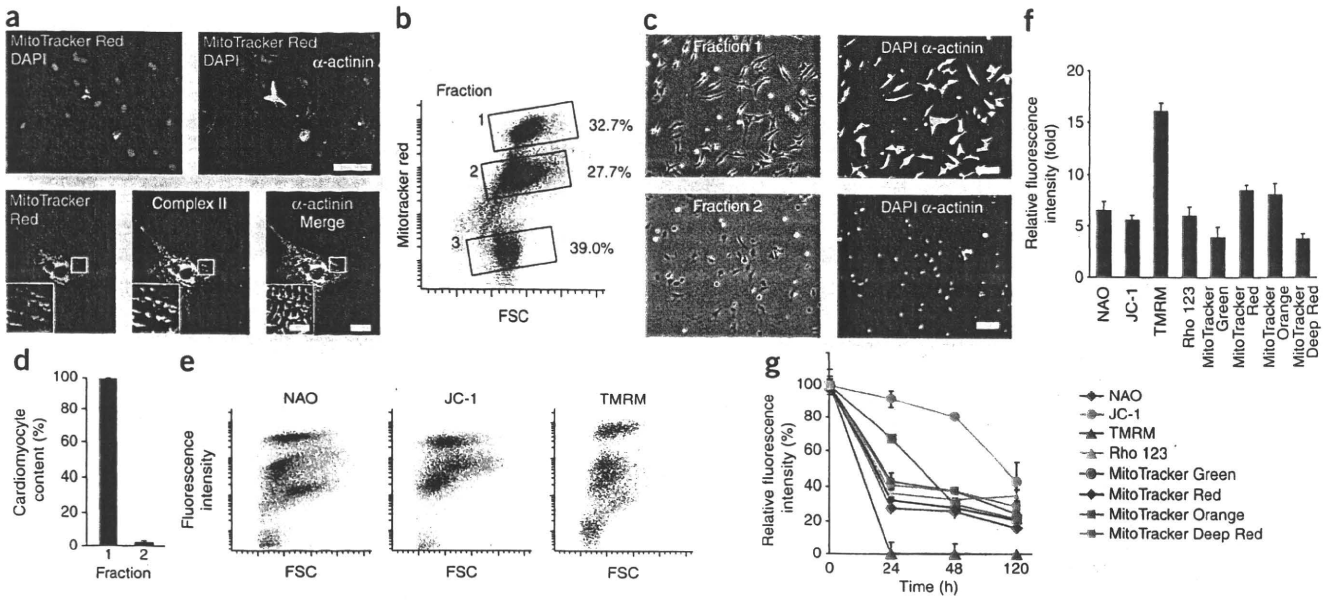

Figure 1 | Mitochondrial dyes for cardiomyocyte purification. (**a**) Fluorescence images of neonatal rat cardiomyocytes prestained with MitoTracker Red and immunostained for α-actinin (top) or prestained with MitoTracker Red and immunostained for mitochondrial electron transfer chain complex II (complex II) and α-actinin (bottom). DAPI, nuclear stain. Scale bars, 100 μm (top); 20 μm (bottom); and 10 μm (bottom inset). (**b**) FACS analysis of neonatal rat heart–derived cells stained with MitoTracker Red. The sorted cells were divided into fractions 1–3 (boxed). FSC, forward scatter. (**c**) Immunofluorescence staining for α-actinin of cells from fractions 1 and 2. Blue, DAPI staining. Scale bars, 100 μm. (**d**) Cardiomyocyte content in fractions 1 and 2. Data are shown as mean ± s.d. (n = 3). (**e**) Representative FACS plots of dissociated cells from neonatal rat heart stained with mitochondrial dyes. (**f**) Relative fluorescence intensity of the indicated mitochondrial dyes in fractions 1 versus 2. Data are shown as mean ± s.d. (n = 3). (**g**) Washout of the indicated mitochondrial dyes from neonatal rat cardiomyocytes. Data are shown as mean ± s.d. (n = 3).

other dyes remained for at least 5 d (**Fig. 1g** and **Supplementary Fig. 3a**). TMRM and JC-1 at 100 nM did not affect cell viability using 3-(4,5-dimethyl-thiazol-2-yl)-2,5-diphenyltetrazolium bromide (MTT) assay, whereas other dyes affected viability differently (**Supplementary Fig. 3b**). Based on these results, we selected TMRM for subsequent experiments.

Purification of cardiomyocytes from heart and whole embryos

To investigate the mitochondrial content of cardiomyocytes at different developmental stages, we performed FACS analysis of rat hearts at embryonic day 11.5 (E11.5) to postnatal day 8 (P8); the hearts had been dissociated and labeled with TMRM (**Fig. 2a**). The mean ratio of TMRM fluorescence in fraction 1 to fraction 2 gradually increased with increasing embryonic stage and rapidly after birth (**Fig. 2b**). FACS analysis followed by immunofluorescence staining confirmed over 99% cardiomyocyte purity at all stages (**Fig. 2c,d**).

We then stained live embryos (E11.5 and E12.5) with TMRM. The heart showed markedly stronger fluorescence compared with other tissues (**Fig. 2e** and **Supplementary Video 1**). Intraplacental injection of MitoTracker Red also resulted in the strongest accumulation of fluorescence in the heart via embryonic circulation. However, other tissues had much weaker fluorescence (**Supplementary Fig. 4**).

To assess why there was strong TMRM fluorescence in the embryonic heart, we compared expression levels of complex I–V of the 36 kDa mitochondrial outer membrane protein porin (also known as the voltage-dependent anion channel) and of heat shock protein 70 between cardiac and various noncardiac tissues in rat E12.5 embryos; we detected markedly stronger expression in the myocardium (**Supplementary Fig. 5**). Furthermore, immunostaining of the fetal heart area for α-actinin, manganese superoxide dismutase (MnSOD) and platelet endothelial cell adhesion molecule (PECAM) (markers of cardiomyocytes, mitochondria and the endothelium, respectively), revealed that MnSOD immunostaining overlapped that for α-actinin but not for PECAM (**Fig. 2f**). Taken together, the accumulation of fluorescent dyes that label mitochondria may reflect high mitochondria abundance in the heart.

Next, we treated dissociated cells obtained from E11.5 to E13.5 whole rat embryos with TMRM and analyzed them on a FACS (**Fig. 2g**). Some cells in this preparation were autofluorescent, which was due to the presence of lipopigments and flavins[13]. To obtain only TMRM-fluorescent cells and eliminate contamination by autofluorescent cells, we adopted pseudo-two-dimensional separation (**Fig. 2g** and Online Methods). We isolated populations with the highest TMRM-fluorescence from dispersed cells of E11.5, E12.5 and E13.5 whole rat embryos. The sorted cells from E11.5 embryos were immunostained for α-actinin (purity 99%, n = 3 embryos; yield, ~5 × 10^3 cells per embryo). We obtained similar results with E12.5 and E13.5 embryos. At these embryonic stages (E11.5–E13.5), the embryos contain skeletal myoblasts only and not mature myotubes. We found that mature skeletal myotubes, which could not pass through the FACS, could be marked with TMRM, whereas skeletal myoblasts, which do pass through the FACS, were not marked by TMRM (**Supplementary Fig. 6**).

Purification of PSC-derived cardiomyocytes

We first observed cardiomyocytes differentiated from mouse ESCs on day 7 of differentiation; the cells had marked TMRM accumulation. After TMRM staining, we fixed the cells and immunostained them for Nkx2.5 and α-actinin (**Fig. 3a**). The Nkx2.5– and α-actinin–positive areas and TMRM-positive area in the mouse

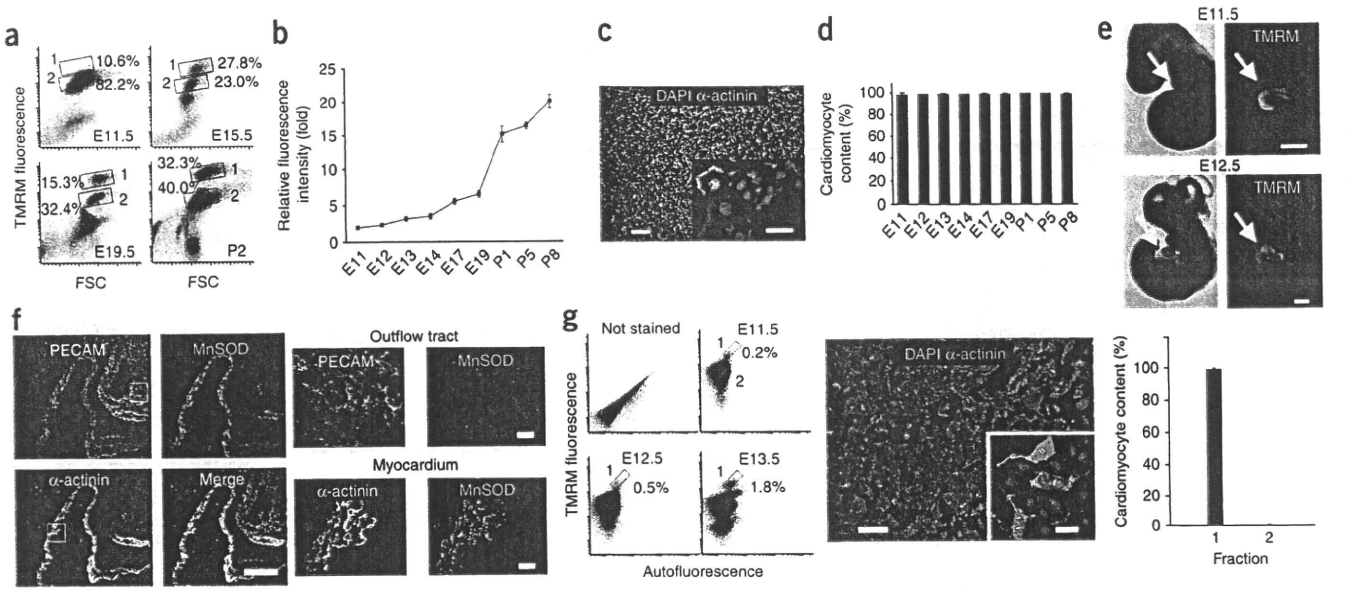

Figure 2 | Purification of cardiomyocytes from embryonic heart and whole embryo. (**a**) Representative FACS analysis of TMRM-stained rat embryonic heart cells at the indicated ages. Fractions 1 and 2 were typical gates for cardiomyocytes and noncardiomyocytes, respectively. (**b**) Relative fluorescence intensity of fraction 1 versus fraction 2 in the developing rat heart. Data are shown as mean ± s.d. (n = 3). (**c**) Immunofluorescence staining for α-actinin in the fraction 1 gated cells from E11.5 rat heart. (**d**) Cardiomyocyte content of the fraction 1-gated cells obtained from E11.5–P8 rat hearts. Data are shown as mean ± s.d. (n = 3). (**e**) Bright field (left) and fluorescence (right) images of whole rat embryos of indicated ages. (**f**) Immunofluorescence staining of rat E11.5 embryo for the indicated markers, PECAM, α-actinin and MnSOD. Images show pericardiac area (left four) and magnification of the boxed areas is shown on the right. (**g**) FACS analysis (left) of dissociated cells from whole embryos in the absence (not stained) or presence of TMRM at the indicated stages. Boxes indicate fractions 1 and 2; percentages of fraction 1 cells are shown. Immunofluorescence staining (middle) for α-actinin in the cells obtained from fraction 1 of E11.5 embryos. Cardiomyocyte content of fractions 1 and 2 at E11.5 is shown (right). Data are shown as mean ± s.d. (n = 3). Scale bars, 100 μm (**c**,**g**,**e**); 200 μm (**f** left); and 20 μm (**c** inset, **f** right, **g** inset).

ESC–derived cardiomyocytes were colocalized completely, although the intracellular localization of TMRM, Nkx2.5 and α-actinin was clearly different. Notably, TMRM dissociated rapidly into the bulk solution compared with other dyes upon fixation (**Supplementary Fig. 7**), indicating that there is likely to be no effect of TMRM on subsequent immunohistochemical analysis.

We applied pseudo–two-dimensional FACS analysis to the embryoid body–derived cells (**Fig. 3b**). We first observed fraction 1 cells 7 d after embryoid body formation. Both the ratio of the mean TMRM fluorescence in fraction 1 (cardiomyocytes) to fraction 2 (noncardiomyocytes) and the percentage of cells in fraction 1 increased gradually until day 15 (**Fig. 3c,d**), suggesting that the best time for obtaining mouse ESC–derived cardiomyocytes was at day 15.

We sorted approximately 5×10^5 to 9×10^5 cells from day 15 embryoid bodies. The viability of the sorted cells was 99.1 ± 1.5%, as confirmed by trypan blue staining (**Supplementary Fig. 8**). This high viability may be due to the fact that the cells were sorted based on TMRM accumulation (and thus contained active mitochondria). We cultured the sorted cells for 7 d to allow the cells to attach to the substrate and to elongate (Online Methods). Immunofluorescence staining for α-actinin and Nkx2.5 in three independent experiments confirmed that these cells were high-purity cardiomyocytes (99.5 ± 0.3%; **Fig. 3e**). We obtained >99% pure ESC-derived cardiomyocytes from day 12–25 embryoid bodies (**Fig. 3f**). We also obtained highly pure cardiomyocytes from mouse iPSCs (**Fig. 3g,h**).

To investigate the possibility of isolating cardiac progenitor cells, we stained whole E7.5 and E7.75 embryos. We found that TMRM faintly, but distinctly, marked the cardiac crescent, which contains cardiomyogenic precursor cells, indicating a possible applicability of our method to obtaining progenitor cells. Next, we carried out time-lapse fluorescence microscopy on attached mouse embryoid bodies stained with TMRM (**Supplementary Fig. 9**). We first observed TMRM-positive cells on day 6.5. Fluorescence in these cells increased gradually between days 6.5 and 7 and they started beating on day 7.0. In contrast, TMRM-negative cells did not beat during the experiments. We then performed FACS analysis on dissociated cells obtained from day 3–6.5 embryoid bodies and stained with TMRM. There were no cells in fraction 1. The higher TMRM-fluorescence cells in fraction 2 from day 3 and 4 embryoid bodies did not differentiate into cardiomyocytes, even after subsequent culture of attached cells for up to 8 d. In the case of day 6.5 embryoid bodies, some of the isolated cells differentiated into cardiomyocytes upon subsequent culture for 3 d. We also stained *Nkx2.5-GFP* knock-in mouse ESCs[6], which we and others have used frequently to isolate cardiomyocytes. After embryoid body formation, we first observed GFP fluorescence on day 7, whereas we observed TMRM staining on day 6.5 (**Supplementary Fig. 10**). Our observations indicate that our method can be used to purify differentiated cardiomyocytes but not cardiac progenitor cells.

We differentiated common marmoset ESCs, human ESCs and human iPSCs into cardiomyocyte-containing embryoid bodies by conventional floating cell culture. We transferred the embryoid bodies into the cell-attachment dishes with 10 nM TMRM. Beating embryoid bodies had extremely high TMRM fluorescence compared with that of nonbeating embryoid bodies derived from marmoset and human ESCs (**Fig. 4a**). Then we dispersed embryoid body–derived cells, stained them with TMRM and analyzed them on a FACS (**Fig. 4b**). We fixed sorted human

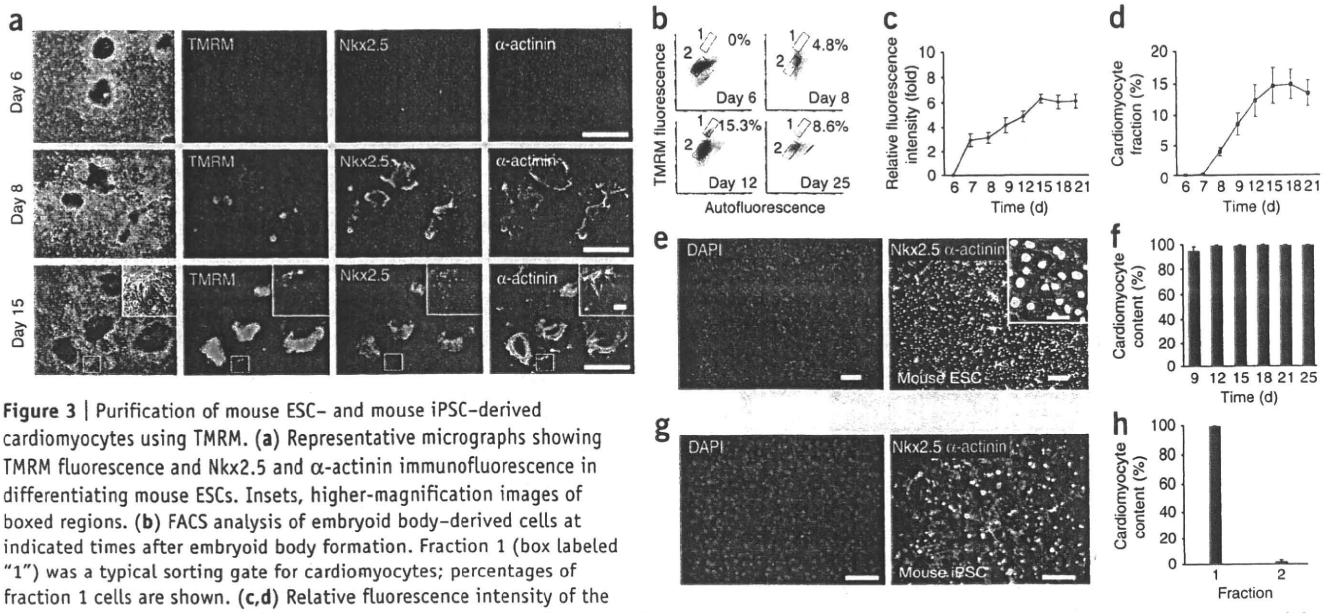

Figure 3 | Purification of mouse ESC- and mouse iPSC-derived cardiomyocytes using TMRM. (**a**) Representative micrographs showing TMRM fluorescence and Nkx2.5 and α-actinin immunofluorescence in differentiating mouse ESCs. Insets, higher-magnification images of boxed regions. (**b**) FACS analysis of embryoid body–derived cells at indicated times after embryoid body formation. Fraction 1 (box labeled "1") was a typical sorting gate for cardiomyocytes; percentages of fraction 1 cells are shown. (**c**,**d**) Relative fluorescence intensity of the fraction 1 versus fraction 2 cells (**c**) and percentage of cells in fraction 1 (**d**) over time. Data are mean ± s.d. (n = 3). (**e**–**h**) Immunofluorescence staining for Nkx2.5 and α-actinin in cultured fraction 1 cells sorted from day 15 embryoid bodies differentiated from mouse ESCs (**e**) and from mouse iPSCs (**g**); and cardiomyocyte content in cultured cells sorted from day 9–25 embryoid bodies differentiated from mouse ESCs (**f**) and in cultured cells sorted from day 15 embryoid bodies differentiated from mouse iPSCs (**h**). Data are mean ± s.d. (n = 3). Scale bars, 1 mm (**a**); and 100 μm (**a** inset, **e**,**g**).

cells in fraction 1, immunostained them for Nkx2.5 and subjected them to a second FACS analysis. The results showed that over 99.9% of cells in fraction 1 were cardiomyocytes (**Fig. 4c**). Furthermore, we compared expression of cardiac and noncardiac genes in human ESC–derived cardiomyocytes isolated by our method and in unpurified cells from embryoid bodies using real-time PCR. We observed a marked increase in the expression of myocardial genes and a decrease in the expression of nonmyocardial genes in purified human ESC–derived cardiomyocytes (**Supplementary Fig. 11**).

We also cultured the sorted cells for 5 d and immunostained them for Nkx2.5 and α-actinin (**Fig. 4d**). Common marmoset ESC, human ESC and human iPSC fraction 1 comprised 99.0 ± 1.0%, 99.0 ± 0.9% and 99.3 ± 0.2% cardiomyocytes, respectively; in contrast, fraction 2 had 2.3 ± 0.6%, 2.5 ± 0.2% and 1.7 ± 1.6% cardiomyocytes, respectively (**Fig. 4e**). To estimate the acquisition efficiency in the sorting experiments, we compared by FACS analysis the cardiomyocyte fraction obtained by TMRM with that obtained by immunofluorescence staining for α-actinin. The number of cardiomyocytes isolated by TMRM staining was 60–90% of the number defined by α-actinin staining (**Supplementary Fig. 12**). To rule out the possibility of skeletal muscle contamination in the sorted cardiomyocyte population, we extracted total mRNA from sorted cardiomyocytes and evaluated it for *myoD* expression using real-time PCR. We confirmed that there was no amplification of *myoD* (**Supplementary Fig. 13**).

No teratoma formation

We cultured the purified mouse ESC-derived cardiomyocytes and noncardiomyocytes for 7 d and found that although noncardiomyocytes formed piled-up colonies, in which some cells

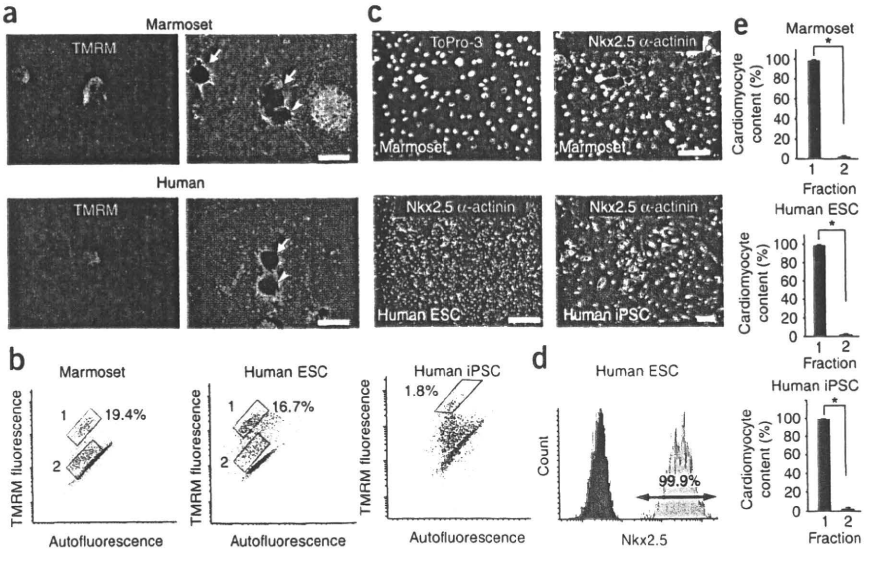

Figure 4 | Purification of PSC-derived cardiomyocytes in human and marmoset. (**a**) TMRM fluorescence (left) and phase contrast (right) images of marmoset and human embryoid bodies containing beating cardiomyocytes. Arrows, beating areas; arrowheads, nonbeating areas. (**b**) FACS separation of TMRM-stained cardiomyocytes derived from common marmoset ESCs, human ESCs and human iPSCs. Fractions 1 and 2 are boxed; percentages of fraction 1 cells are shown. (**c**) Immunofluorescence staining of fraction 1 cells for α-actinin and Nkx2.5. ToPro-3 represents nuclear staining. (**d**) Histogram showing immunodetection of Nkx2.5 (gray) and negative control (without first antibody; black) in sorted human ESC–derived fraction 1 cells. (**e**) The cardiomyocyte content of fractions 1 and 2 in common marmoset ESCs, human ESCs and human iPSCs. Data are mean ± s.d. (n = 3). *P < 0.01 (Student t-test). Scale bars, 500 μm (**a**); and 100 μm (**c**).

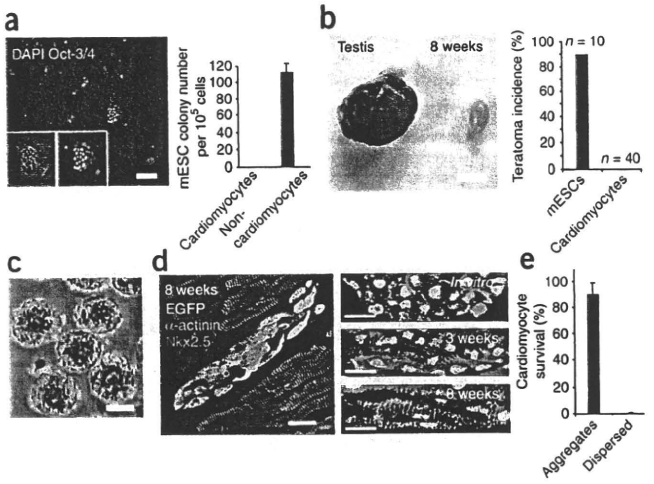

Figure 5 | Transplantation of purified mouse ESC-derived cardiomyocytes. (**a**) Immunofluorescence staining for Oct3/4 (red) in the sorted cells from the noncardiac fraction (left), and numbers of mouse ESC-like colonies obtained from 10^5 sorted cells (right). Data are mean ± s.d. (n = 3). (**b**) Transplantation of 250 undifferentiated mouse ESCs into testes resulted in teratoma formation (testis), whereas transplantation of 1.9×10^5 purified mouse ESC-derived cardiomyocytes did not (8 weeks). Incidence of teratoma formation was quantified (right). (**c**) Phase contrast image of mouse cardiomyocyte aggregates. (**d**) Immunofluorescence staining of engrafted mouse cardiomyocyte aggregates for α-actinin and Nkx2.5 8 weeks after transplantation (left); transplanted cells expressed EGFP. Mouse ESC-derived cardiomyocytes *in vitro* and 3 and 8 weeks after transplantation immunostained for Nkx2.5 and α-actinin (right). (**e**) Transplanted mouse ESC-derived cardiomyocyte survival. Data are shown as mean ± s.d. (n = 5). Scale bars, 100 μm (**a**,**c**); 5 mm (**b**); and 20 μm (**d**).

were positive for Oct3/4, the cardiomyocytes did not (**Fig. 5a**). Further, we transplanted 1.9×10^5 aggregated mouse ESC–derived cardiomyocytes and 250 undifferentiated mouse ESCs as a control into the testes of immunocompromised nonobese diabetic–severe combined immunodeficient (NOD-SCID) mice. Two months later, 90% of the control mice developed teratomas (9 of 10 mice), but we did not detect teratomas in any of the mice transplanted with purified mouse ESC–derived cardiomyocytes (0 of 40 mice) (**Fig. 5b**). We tried to verify that there was no teratoma formation in the heart by directly injecting mouse ESC–derived cardiomyocytes (1×10^5) into the myocardium of five NOD-SCID mice immediately after sorting. Two months later, we found few (<1%) of the transplanted cardiomyocytes in the heart (data not shown).

To understand the mechanism underlying this cell loss, we injected purified and MitoTracker Red–labeled neonatal rat cardiomyocytes into the left ventricular free wall of *ex vivo*–perfused hearts. We found one-third to one-half of injected cells in the postperfusion solution, indicating that the neonatal rat cardiomyocytes were washed out within the first 10 min (**Supplementary Fig. 14**). Next, we compared the tissue adhesiveness of purified mouse ESC–derived cardiomyocytes and mouse embryonic fibroblasts (MEFs) by counting cells in continuous sections of whole ventricles 24 h after injection into the left ventricular free walls. We found that less than 1% of the grafted ESC-derived cardiomyocytes had adhered to the host myocardium, compared with 50% of MEFs.

Transplantation of PSC-derived cardiomyocytes

From the above observations, we reasoned that loss of transplanted ESC-derived cardiomyocytes may be due to rapid washout and low adhesiveness of the cells. Because ESC-derived cardiomyocytes existed as homophilic cell aggregates (diameter, 100–500 μm) in mouse, marmoset and human embryoid bodies (**Supplementary Fig. 15**), we suspected that re-aggregated purified ESC-derived cardiomyocytes may be more resistant to rapid washout. We generated cardiomyocyte aggregates by seeding 313–10,000 purified mouse ESC–derived cardiomyocytes onto nonadhesive 96-well plates. One day after seeding, the cells adhered to each other, aggregated and started synchronized beating; 5 d later, cardiomyocyte aggregates formed with diameters of 100–450 μm (**Fig. 5c**, **Supplementary Fig. 16** and **Supplementary Video 2**). Propidium iodide staining revealed that a high proportion of re-aggregated mouse ESC–derived cardiomyocytes were viable (98.8 ± 0.2% of seeded cells; **Supplementary Fig. 16**).

We transplanted mouse cardiomyocyte aggregates into the ventricular free walls of NOD-SCID mice and killed the mice at 3 and 8 weeks (n = 5 for both groups). We observed no teratoma formation in either group. Immunofluorescence staining revealed that cell aggregates positive for the tracers Nkx2.5 and α-actinin were located in the left ventricle (**Fig. 5d**). The number of cells that survived in the heart was greater than 90% (**Fig. 5e**). Furthermore, we repeated these experimental procedures using purified human ESC–derived cardiomyocytes (**Supplementary Video 3**). Two months after transplantation, we detected a large amount of human myocardial tissue in NOD-SCID mouse heart (**Supplementary Fig. 17**).

Finally, we investigated which autoparacrine factors are important for the survival of ESC-derived cardiomyocytes. Human cardiomyocyte aggregates remained viable under serum-free culture conditions; moreover, their diameters increased by approximately twofold by day 25. Supplementation of the cultures with physiological concentrations of basic fibroblast growth factor (bFGF), epidermal growth factor (EGF), platelet-derived growth factor beta dimer (PDGF-BB) and endothelin-1 (ET-1) strongly enhanced the growth of the cardiomyocyte aggregates (**Supplementary Fig. 18a** and **Supplementary Video 4**). We confirmed expression of these growth factors and their receptors by real-time PCR (probe and primer sets are listed in **Supplementary Table 1**). We also confirmed that these growth factors were expressed in adult human and mouse hearts (**Supplementary Fig. 18b**). Autoparacrine stimulation with these growth factors may be one reason why grafted cardiomyocyte aggregates survived and grew in the host myocardium.

DISCUSSION

Our method for cardiomyocyte isolation has two advantages. First, it does not require genetic modification of the cells. Genetic modifications using nonviral or viral systems have several disadvantages: extrinsic genes may be silenced, the number of integration events in one cell is difficult to control, targeted integration is not straightforward, and line selection as well as verification of proper expression of extrinsic genes[14] is time-consuming. Furthermore, genetic modification carries risks such as possible tumor formation[15–17]. Second, our method is likely to be widely applicable. We demonstrated that it may be used to purify ESC-derived cardiomyocytes in four species, including human,

and that it is also applicable to mouse and human iPSCs. High abundance of cellular mitochondria is likely to be a common characteristic of cardiomyocytes irrespective of species. In contrast, most genetic modifications require species-specific constructs. Our simple purification strategy should facilitate basic studies using embryonic heart and stem cell–derived cardiomyocytes; furthermore, this strategy can also allow isolation of noncardiomyocytes, which may open up new approaches to studying developmental interactions.

The ESC-derived cardiomyocytes purified using our method did not induce teratoma formation in either the heart or testes. Although from the viewpoint of clinical safety, further studies using large animal models with a much larger number of ESC-derived cardiomyocytes will be required, we believe that our purification method may have considerable advantages over existing methods for eventual clinical translation as well.

Our results suggest that induction of mitochondrial biogenesis begins shortly before beating of cardiomyocytes. This indicates the tight relationship between cardiomyogenesis and mitochondrial biogenesis. A combination of our strategy and other marking techniques for cardiac progenitor cells may facilitate study in this field.

Unpurified fetal and neonatal rat cardiomyocytes and bone marrow mesenchymal and ESC-derived cardiomyocytes have been shown to survive in the recipient heart[18–20]. In contrast, purified and dispersed cardiomyocytes differentiated from ESCs did not achieve a high survival rate[5]. Re-aggregation augmented the long-term survival of purified mouse and human ESC–derived cardiomyocytes. Our results indicate that ESC-derived cardiomyocytes might be highly anchorage-dependent, and that homophilic cell-to-cell adhesion and autoparacrine signaling may be important factors contributing to their survival.

METHODS

Methods and any associated references are available in the online version of the paper at http://www.nature.com/naturemethods/.

Note: Supplementary information is available on the Nature Methods website.

ACKNOWLEDGMENTS

Human ESCs were a gift of N. Nakatsuji at the Department of Development and Differentiation, Institute for Frontier Medical Sciences, Kyoto University. Human and mouse iPSCs were a gift of S. Yamanaka at the Center for iPS Cell Research and Application, Institute for Integrated Cell-Material Sciences, Kyoto University. Mouse ESCs were a gift of H. Niwa at the Laboratory of Pluripotent Cell Studies, RIKEN Center for Developmental Biology. This study was supported in part by research grants from the Ministry of Education, Science and Culture, Japan, and by the Program for Promotion of Fundamental Studies in Health Science of the National Institute of Biomedical Innovation.

AUTHOR CONTRIBUTIONS

F.H. designed the whole study. F.H. performed most experiments and wrote the manuscript. H.C. participated in cell-sorting experiments and prepared cells. H.Yamashita participated in cell-sorting experiments, PCR experiments, immunofluorescent staining, animal experiments and preparing cells. S.T., Y.S., W.L., T.T., T.O., K.S., Y.O. and T.E. participated in cell preparations. H.Yamakawa and M.M. participated in heart perfusion experiments. K.H. and T.M. provided the *Nkx2.5 knock-in* ESCs. S.Y., M.M., R.K., M.S., S.M. and S.O. provided advice. E.S. provided cmESCs. T.S. supervised Y.S. K.F. provided advice, obtained the budget and supervised the project.

COMPETING INTERESTS STATEMENT

The authors declare competing financial interests: details accompany the full-text HTML version of the paper at http://www.nature.com/naturemethods/.

Published online at http://www.nature.com/naturemethods/.
Reprints and permissions information is available online at http://npg.nature.com/reprintsandpermissions/.

1. Yuasa, S. *et al.* Transient inhibition of BMP signaling by Noggin induces cardiomyocyte differentiation of mouse embryonic stem cells. *Nat. Biotechnol.* **23**, 607–611 (2005).
2. Nemir, M., Croquelois, A., Pedrazzini, T. & Radtke, F. Induction of cardiogenesis in embryonic stem cells via downregulation of Notch1 signaling. *Circ. Res.* **98**, 1471–1478 (2006).
3. Mummery, C. *et al.* Differentiation of human embryonic stem cells to cardiomyocytes: role of coculture with visceral endoderm-like cells. *Circulation* **107**, 2733–2740 (2003).
4. Anderson, D. *et al.* Transgenic enrichment of cardiomyocytes from human embryonic stem cells. *Mol. Ther.* **15**, 2027–2036 (2007).
5. Kolossov, E. *et al.* Engraftment of engineered ES cell-derived cardiomyocytes but not BM cells restores contractile function to the infarcted myocardium. *J. Exp. Med.* **203**, 2315–2327 (2006).
6. Hidaka, K. *et al.* Chamber-specific differentiation of Nkx2.5-positive cardiac precursor cells from murine embryonic stem cells. *FASEB J.* **17**, 740–742 (2003).
7. Fijnvandraat, A.C. *et al.* Cardiomyocytes purified from differentiated embryonic stem cells exhibit characteristics of early chamber myocardium. *J. Mol. Cell. Cardiol.* **35**, 1461–1472 (2003).
8. Gassanov, N., Er, F., Zagidullin, N. & Hoppe, U.C. Endothelin induces differentiation of ANP-EGFP expressing embryonic stem cells towards a pacemaker phenotype. *FASEB J.* **18**, 1710–1712 (2004).
9. Huber, I. *et al.* Identification and selection of cardiomyocytes during human embryonic stem cell differentiation. *FASEB J.* **21**, 2551–2563 (2007).
10. Klug, M.G., Soonpaa, M.H., Koh, G.Y. & Field, L.J. Genetically selected cardiomyocytes from differentiating embronic stem cells form stable intracardiac grafts. *J. Clin. Invest.* **98**, 216–224 (1996).
11. Laflamme, M.A. *et al.* Cardiomyocytes derived from human embryonic stem cells in pro-survival factors enhance function of infarcted rat hearts. *Nat. Biotechnol.* **25**, 1015–1024 (2007).
12. Xu, C., Police, S., Hassanipour, M. & Gold, J.D. Cardiac bodies: a novel culture method for enrichment of cardiomyocytes derived from human embryonic stem cells. *Stem Cells Dev.* **15**, 631–639 (2006).
13. Monici, M. Cell and tissue autofluorescence research and diagnostic applications. *Biotechnol. Annu. Rev.* **11**, 227–256 (2005).
14. Gropp, M. & Reubinoff, B. Lentiviral vector-mediated gene delivery into human embryonic stem cells. *Methods Enzymol.* **420**, 64–81 (2006).
15. Tsukahara, T. *et al.* Murine leukemia virus vector integration favors promoter regions and regional hot spots in a human T-cell line. *Biochem. Biophys. Res. Commun.* **345**, 1099–1107 (2006).
16. Recchia, A. *et al.* Retroviral vector integration deregulates gene expression but has no consequence on the biology and function of transplanted T cells. *Proc. Natl. Acad. Sci. USA* **103**, 1457–1462 (2006).
17. Woods, N.B. *et al.* Lentiviral vector transduction of NOD/SCID repopulating cells results in multiple vector integrations per transduced cell: risk of insertional mutagenesis. *Blood* **101**, 1284–1289 (2003).
18. van Laake, L.W. *et al.* Human embryonic stem cell-derived cardiomyocytes survive and mature in the mouse heart and transiently improve function after myocardial infarction. *Stem Cell Rev.* **1**, 9–24 (2007).
19. Reinecke, H., Zhang, M., Bartosek, T. & Murry, C.E. Survival, integration, and differentiation of cardiomyocyte grafts: a study in normal and injured rat hearts. *Circulation* **100**, 193–202 (1999).
20. Hattan, N. *et al.* Purified cardiomyocytes from bone marrow mesenchymal stem cells produce stable intracardiac grafts in mice. *Cardiovasc. Res.* **65**, 334–344 (2005).

Int. J. Dev. Biol. 53: 615-622 (2009)
doi: 10.1387/ijdb.092850mh

THE INTERNATIONAL JOURNAL OF DEVELOPMENTAL BIOLOGY
www.intjdevbiol.com

A novel *in vitro* system for studying cardiomyocyte differentiation with medaka embryonic cells

MASAO HYODO*[,1], SHINJI MAKINO[2], YASUNORI AWAJI[1], YOHEI SAKURADA[1], TOMOICHI OHKUBO[3], MITSUSHIGE MURATA[2], KEIICHI FUKUDA[2] and MICHIO TSUDA[4]

[1]*Department of Biological Science and Technology, Tokai University, Numazu, Japan,* [2]*Department of Regenerative Medicine and Advanced Cardiac Therapeutics, Keio University School of Medicine, Shinjuku, Tokyo, Japan,* [3]*Teaching and Research Support Center, and* [4]*Department of Molecular Life Science, Tokai University School of Medicine, Boseidai, Isehara, Japan*

ABSTRACT Our studies revealed that dissociated cells from medaka (the fresh-water fish, *Oryzias latipes*) blastula-stage embryos differentiate into many rhythmically contracting cells when incubated with a conditioned medium from a cell line. Analyses of these cells by immunostaining, electron microscopy, expression of marker genes, action potential recordings and pharmacological responses all showed the characteristics of myocardial cells. We succeeded in purifying the cardiac cell-inducing factor from the conditioned medium by 523,100-fold with 8% recovery of the protein. Analysis of its amino-acid sequence by mass spectrometry revealed the factor to be medaka activin A_2 (homodimer of inhibin βA_2 subunit). Recombinant human activin A showed the same cardiac cell-inducing activity toward medaka embryonic cells. Our results demonstrate that activin A is a potent factor for medaka myocardial cell differentiation. This culture method should provide a novel and simple experimental system to study cardiomyocyte differentiation *in vitro*.

KEY WORDS: *medaka, activin, cardiomyocyte, embryonic cell culture*

Introduction

Pluripotent embryonic stem (ES) cell lines have been established from the inner cell masses of early human (Thomson *et al.*, 1998) or other mammalian embryos and are expected to provide a unique system for tissue engineering. The technology to induce pluripotent stem cells (the iPS cells) from cultured mouse (Takahashi and Yamanaka, 2006) or human (Takahashi *et al.*, 2007) somatic cells has recently been developed. Thus it will be possible to create pluripotent cells directly from somatic cells of patients. Differentiation of ES or iPS cells into cardiomyocytes has been demonstrated (Kehat *et al.*, 2001; Xu *et al.*, 2002; Passier *et al.*, 2005; Denning *et al.*, 2006; Laflamme *et al.*, 2007; Takahashi *et al.*, 2007). Attempts to treat heart disease using these cells have been carried out and transplantation of human ES cell-derived cardiomyocytes to infarcted hearts of athymic rat or mouse was shown to improve heart function (Laflamme *et al.*, 2007; van Laakea *et al.*, 2007). While these methods are expected to be used in regenerative cell therapy for treatment of human heart disease, more detailed studies are required for a better understanding of the molecular mechanisms of early cardiac differentiation, proliferation and maturation of the induced cardiomyocytes.

The protocol for *in vitro* induction of the cardiomyocytes was based on the results of experiments using animal models such as amphibians and chicken. Experiments with tissue fragments from embryos of these animals revealed that cardiac myogenesis is regulated by several temporally and spatially distinct signaling events. Although participation of many protein factors has been reported in cardiogenesis including activin, bone morphogenetic proteins (BMPs), or fibroblast growth factors (FGFs) (Lough and Sugi, 2000; Yutzey and Kirby, 2002; Zaffran and Frasch, 2002; Brand, 2003; Fukuda and Yuasa, 2006), the primary mechanisms underlying cardiac induction, especially which signal initiates specification, have yet to be fully characterized. In chicken embryos, there seem to be distinct mechanisms between the cardiac cell-inducing activities of early stage hypoblasts and those of late stage antero-lateral (AL) endo-

Abbreviations used in this paper: AL- antero-lateral; BMP, bone morphogenetic protein; CM, conditioned medium; ES, embryonic stem.

***Address correspondence to:** Masao Hyodo. Department of Biological Science and Technology, Tokai University, Numazu, 410-0395, Japan. Fax: +81-55-968-1156. e-mail address: hyodo@tokai.ac.jp

Supplementary Material for this paper (a movie) is available at: http://dx.doi.org/10.1387/ijdb.092850mh

Accepted: 1 December 2008. *Published online:* 23 January 2009. *Edited by:* Makoto Asashima.

ISSN: Online 1696-3547, Print 0214-6282

derm where hypoblast-derived signals (activin) act upstream of the heart-inducing signals provided by AL endoderm (BMPs and FGFs) (Sugi and Lough, 1995; Schultheiss *et al.*, 1995; Lough *et al.*, 1996; Yatskievych *et al.*, 1997; Ladd *et al.*, 1998; Barron *et al.*, 2000). In frog embryos, induced differentiation of animal cap cells into cardiomyocytes *in vitro* was shown after treatment with activin (Ariizumi *et al.*, 1996; Ariizumi *et al.*, 2003).

Small fresh-water fish such as medaka *(Oryzias latipes)* and zebrafish *(Danio rerio)* are attracting increasing interest as animal models for research in vertebrate development. We have been using pluripotent cells isolated from early stage medaka embryos for cell culture experiments (Hyodo *et al.*, 1998). Medaka produces considerable numbers of eggs daily under conditions of controlled water temperature and light periods. The eggs are relatively large (about 1 mm in diameter) and transparent so that they can be easily observed or manipulated under low magnification microscopy. The recent release of a draft genome sequence for medaka should facilitate research in many fields (Kasahara *et al.*, 2007). Although attempts to establish ES cells from fish embryos have been reported (Hong *et al.*, 1998; Fan and Collodi, 2006), success remains limited. Furthermore, there have been no reports of studies employing *in vitro* fish cell culture to investigate the induction of cardiomyocytes. During our study to culture medaka embryonic cells, we found that a conditioned medium prepared with a medaka cell line effectively induces cardiogenesis *in vitro*. We report here the purification and identification of the protein factor responsible for this induction. The factor was found to be medaka activin A_2. Human activin A was also shown to have cardiac cell-inducing activity in this new experimental system.

Results

Induction of rhythmically contracting cells from medaka embryonic cells

While we were attempting to establish ES cells from medaka embryos (Hyodo *et al.*, 1998), we tested the effect of the conditioned medium. The conditioned media were prepared from 6 medaka fibroblast cell lines established independently in our laboratory. They were added to cultures of dissociated cells prepared from the blastula-stage medaka embryos. Then we found that one of them (CM-1) induced spontaneously contracting cells after several days of incubation. Differentiation occurred in primary cultures in which most of the cells were growing as a monolayer.

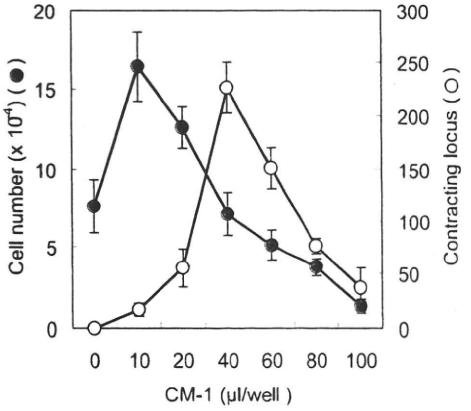

Fig. 1. Dose-dependent effects of the conditioned medium (CM-1) on the cell growth and cardiac differentiation of medaka embryonic cells. *Closed circles: number of cells/well. Open circles: number of contracting loci/well. Values represent mean ± SE (n = 5-7).*

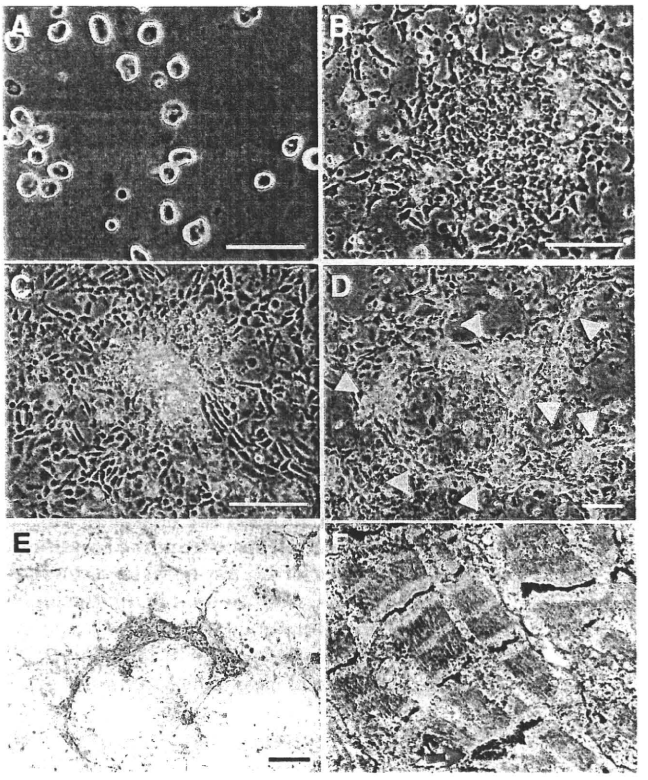

Fig. 2. Differentiation of cardiomyocytes from medaka embryonic cells dissociated at the blastula stage. (A-E) *Light microscopic observation.* **(A)** *Cells dissociated from blastula-stage embryos.* **(B)** *Cells incubated for 1 day.* **(C)** *Cells incubated for 2 days. An asterisk indicates apoptotic cells.* **(D)** *Cells incubated for 6 days. Arrowheads indicate contracting loci.* **(E)** *Immuno-histochemical micrograph of cells incubated for 5 days. Scale bar in (A-E), 100 µm.* **(F)** *Transmission electron micrograph of sectioned beating cells after 14 days of incubation. Arrowheads indicate Z-band and an arrow indicates an intercalated disc.*

At first, we examined the dose-dependent effects of CM-1 and the results are shown in Fig. 1. For determination of cardiac cell-inducing activity, the contracting loci (groups of cardiomyocytes) were counted under a microscope after 5 days of incubation. The results show that the differentiation of contracting cells was dependent on CM-1. Without the addition of CM-1, contracting cells were almost never observed. When 10-20 µl of CM-1 was added to the culture, cell growth was promoted and lower level of cardiac differentiation was observed. Then a maximum number of contracting locus was found when 40 µl of CM-1 was added to a 1.2 ml culture. Under the same conditions,

cell number decreased to about 50% of the maximum. When increasing the amount of CM-1 to more than 40 μl/well, extensive cell death occurred so that both the cell number and yield of contracting loci decreased. These results show that differentiation occurred within a narrow concentration range of a factor contained in CM-1.

Characterization of rhythmically contracting cells

Fig. 2 shows a typical result of microscopic observation of cultured medaka embryonic cells. At first, blastoderms were excised from blastula-stage embryos, and blastomeres were dissociated into single cells (Fig. 2A). Cells were then incubated in 1.2 ml of 199ES2 medium containing 40 μl CM-1, the most suitable conditions for differentiation of the contracting cells. After 1 day of incubation, many colonies of epithelial cells were observed (Fig. 2B). The cells were small and each cell contained a large nucleus and a small amount of cytoplasm. At the center of colonies, cells were tightly associated with each other so that the cell boundaries were not clear. Their appearance was similar to those of mammalian ES cells. After incubation for 2 days, some cells at the center of these colonies died and degraded (Fig. 2C). Many of the surviving cells were found to differentiate into rhythmically contracting cells. The cells started beating after incubation for 2-3 days. This beating was weak and irregular at first, but it became regular and strong after 4 days of incubation. In intact embryos, heart contractions started at approximately the same time (Iwamatsu, 2004) as those in the *in vitro* culture system. Fig. 2D shows groups of contracting loci incubated for 6 days. Contracting cells are also shown in the online data supplements (Movie 1). The pulse rate was approximately 100-110/min at 28°C, and this was similar to those of intact embryonic heart. Such rhythmical contractions continued for more than 2 months with weekly medium changes.

To characterize these rhythmically contracting cells, the expression of a cardiac troponin I in cultured cells was investi-

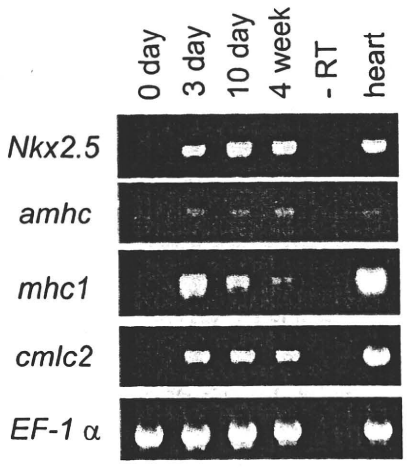

Fig. 3. The expression of 5 genes (*Nkx2.5, amhc, mhc1, cmlc2* and *EF-1α*) was analyzed by RT-PCR. *RNA was extracted from cells immediately after dissociation of the blastoderm (0 day), after incubation of up to 4 weeks, or from the intact medaka heart. In negative control reactions, reverse transcriptase was omitted (-RT).*

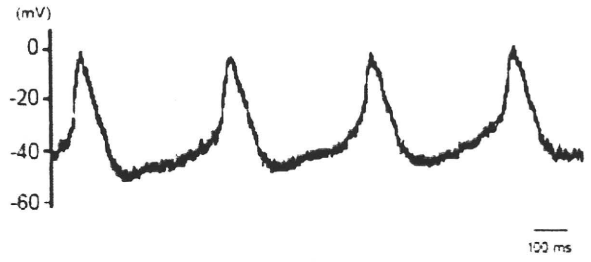

Fig. 4. Electrophysiological analysis of cardiomyocytes differentiated *in vitro*.

gated by immuno-staining with a monoclonal antibody. As shown in Fig. 2E, the contracting loci were positively stained with the anti-cardiac troponin I antibody. Among cells incubated without CM-1, no contracting cells formed and cells were not stained with the monoclonal antibody (data not shown). Fig. 2F shows a result of ultrastructural analysis of embryonic cell-derived beating cells incubated for 14 days. The electron micrograph shows sarcomeric organization with Z-bands and intercalated discs. Thus, the results of immunohistochemical and ultrastructural analyses indicated that the spontaneously contracting cells displayed characteristics of cardiomyocytes.

Fig. 3 shows the results of gene expression analysis by RT-PCR. The expression levels of four cardiac-specific genes, including *Nkx2.5* (cardiac specific homeobox gene), *amhc* (atrium myosin heavy chain), *mhc1* (myosin heavy chain 1), *cmlc2* (cardiac myosin light chain 2), as well as *EF-1α* (elongation factor 1α) as a control, were examined. The results show that expression of the cardiac specific genes can be detected after incubation in CM-1 for 3 days and continues for at least 4 weeks.

An electrophysiological study was carried out on the contracting cells after 2 weeks of incubation in CM-1 (Fig. 4). A cardiomyocyte-like action potential was recorded from these spontaneously beating cells and shows the following properties: (1) a relatively long action potential duration or plateau; (2) a relatively shallow resting membrane potential; and (3) a pacemaker-like late diastolic slow depolarization. They revealed a sinus node-like action potential rather than action potentials like those of matured ventricular cardiomyocytes. These results confirmed that the contracting cells were cardiomyocytes.

Pharmacological responses of the contracting cells

To further characterize the properties of differentiated cardiomyocytes derived from medaka embryonic cells, their pharmacological responses were examined. For this purpose, cardiomyocytes were incubated with various concentrations of drugs and their beating frequencies were measured. The contracting cells were treated with phenylephrine (an α_1- adrenergic receptor agonist; Fig. 5A), or isoproterenol (a β_1- adrenergic receptor agonist; Fig. 5B). Both of these drugs enhanced contraction rate in a dose-dependent manner. Clenbuterol (a β_2-adrenergic receptor agonist; Fig. 5C) caused slight increases in the beating rate. Fig. 5D shows that the beating frequency was decreased by diltiazem (a calcium channel blocker) in a concentration-dependent manner and that treatment of cells

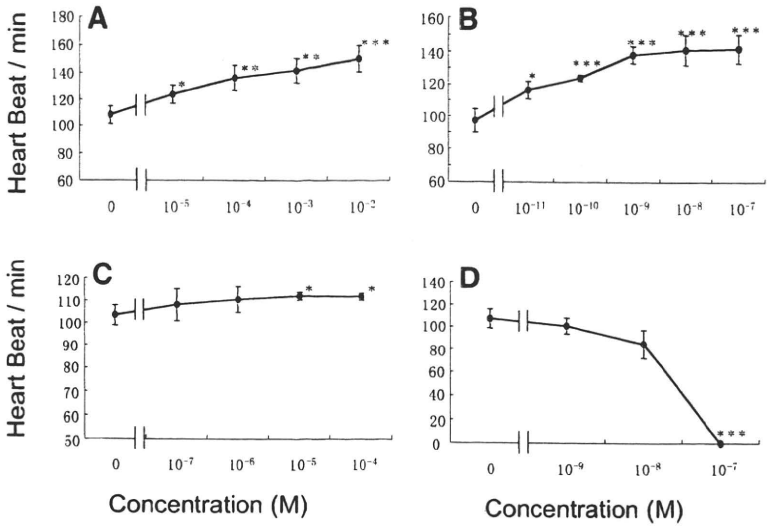

Fig. 5. Study of pharmacological responses with differentiated cardiomyocytes. *Effect of phenylephrine (α_1-adrenoceptor agonist)* **(A)**, *isoproterenol (β_1-adrenoceptor agonist)* **(B)**, *clenbuterol (β_2-adrenoceptor agonist)* **(C)** *and diltiazem (calcium channel blocker)* **(D)** *on medaka cardiomyocytes induced from embryonic cells. Values represent mean ± SE (n = 3-4). * p<0.05, ** p<0.005, *** p<0.001.*

with 10^{-7} M diltiazem stopped contractions completely. These results show that differentiated cardiomyocytes responded to adrenergic agonists and Ca^{2+} blockers similarly to those *in vivo*.

Purification and identification of the cardiac cell-inducing factor

To purify the cardiac cell-inducing factor from the conditioned medium, fractionation steps employing ammonium sulfate, SP-Sephadex, Sephadex G-75, hydroxyapatite and SP-Sepharose columns were performed. For determination of cardiac cell-inducing activity during these steps, one unit was defined as the amount of activity that induces one contracting locus in a well. Using these procedures, the cardiac cell-inducing factor was purified by 523,100-fold with 8% protein recovery from CM-1 (Table 1). The molecular mass of the factor was estimated to be 24-28 kDa by Sephadex G-75 column chromatography (data not shown). Fig. 6 shows a final result of SP-sepharose column chromatography. The activity was detected as a discrete peak at approximately 40 mmol/L NaCl.

For determination of the amino-acid sequence of this factor, the purified protein was digested by trypsin and separated peptides were analyzed by a mass spectrometer (Ultraflex MALDI LIFT TOF/TOF MS, Brukar Daltonics K. K.). Peptide mass fingerprint (PMF) data identified the factor as inhibin βA_2 subunit (EMBL/GenBank/DDJB accession no. AB009408) (Tada *et al.*, 1998). Inhibin is composed of two peptides, α and β subunits, and activin is a homodimer of inhibin β subunits. Since only the inhibin βA_2 subunit was detected, we conclude that the purified cardiac cell-inducing factor is the medaka activin A_2 (βA_2 homodimer). Fig. 7A shows the dose-dependent effects of the purified medaka activin A2 on the dissociated embryonic cells. The results are similar to those with CM-1 (Fig. 1).

Human activin A can induce medaka cardiac myocytes

We next examined whether human activin A (78% identity to medaka activin A_2 in amino-acid sequence) possesses the same cardiac cell-inducing activity towards medaka embryonic cells. The results are shown in Fig. 7B and indicate that recombinant human activin A has the same activity as medaka activin A_2. It promoted cell growth at low concentrations, induced myocardial cell differentiation at medium-range concentrations and caused cell death at higher concentrations. The results in Fig. 7 show that 1 ng/well (0.83 ng/ml) of the medaka activin A_2 can induce ~300 contracting loci, whereas 3 ng/well (2.5 ng/ml) of human activin A can induce ~200 contracting loci. Microscopic observations of cultured cells incubated with human activin A showed them to have morphological appearances indistinguishable from those of cells induced with CM-1 or purified medaka activin A_2.

Then we performed molecular identification of the cardiomyocytes induced by human activin A. The rhythmically contracting cells were positively stained with the anti-cardiac troponin I antibody (Fig. 8). And RT-PCR experiments revealed that expression of the cardiac specific genes can also be detected (Fig. 9). These results confirm that activin A is a potent inducer of myocardial cells from medaka embryonic cells.

Discussion

Differentiation of cardiomyocytes in vitro

We found that when dissociated cells isolated from the medaka blastula-stage embryos were incubated with the conditioned

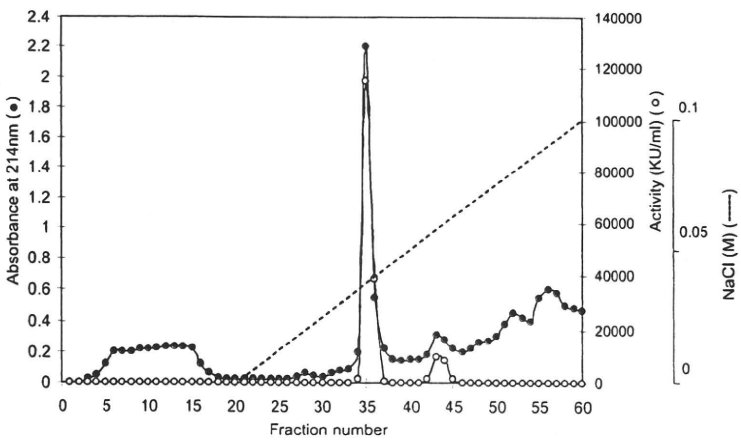

Fig. 6. A profile of the SP-Sepharose column chromatography. *Proteins were eluted with a linear gradient of 0-100 mmol/L NaCl in basal buffer at a flow rate of 0.5 ml/min. Activity was detected as a discrete peak at 40-50 mmol/L NaCl. Open circles: activity of cardiac cell-inducing factor (kilo units/ml). Closed circles: absorbance at 214 nm. Dashed line: NaCl concentration.*

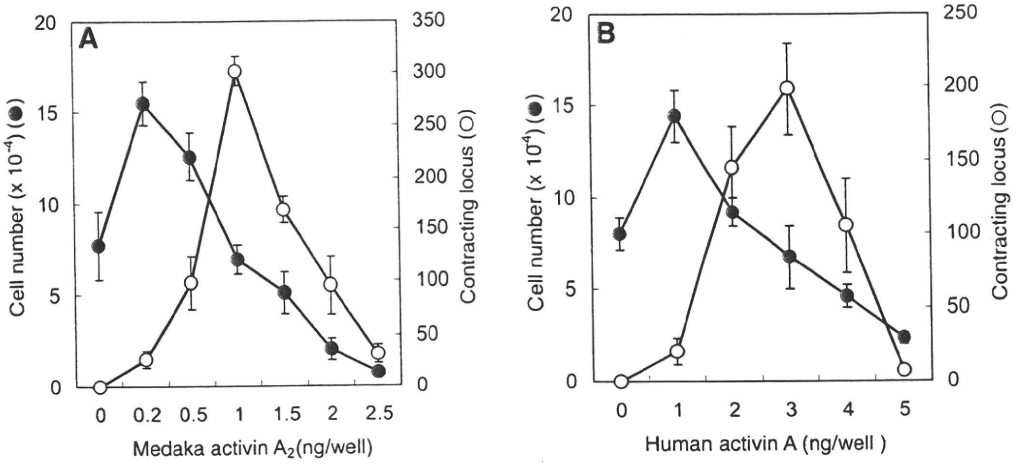

Fig. 7. Effects of the purified medaka activin A_2 (A) and human activin A (B) on the medaka embryonic cells. *Closed circles: number of cells/well. Open circles: number of contracting loci/well. Values represent mean ± SE (n = 4 ~5).*

medium (CM-1), many cells differentiated into rhythmically contracting cells. These cells were characterized as cardiomyocytes. Development of heart has been shown in *in vitro* cultures of avian (Sugi and Lough, 1995; Schultheiss *et al.*, 1995; Lough *et al.*, 1996; Yatskievych *et al.*, 1997; Ladd *et al.*, 1998; Lough and Sugi, 2000; Barron *et al.*, 2000; Yutzey and Kirby, 2002) and amphibian (Ariizumi *et al.*, 2003) embryo explants. In most of these cases, the cells develops into complex structures containing different tissue lineages. In contrast to these results, our study showed that dissociated medaka blastomeres incubated with CM-1 formed monolayer colonies and differentiated into spontaneously contracting cells (Fig. 2). This induction of cardiac differentiation is highly reproducible and the ratio of cardiomyocytes is about 30-40% of the surviving cells as judged by microscopic observation of the intact and immuno-stained cells. Differentiation of myocardial cells was the most significant event in this culture system. The rest of the culture was composed of epithelial or spindle-shaped cells. In some cases, a small number of notochord cells (less than 5% of survived cells) which were composed of typical vacuolized cells, were formed. However, these appeared without CM-1, and addition of CM-1 decreased their number, so that differentiation of notochord occurred spontaneously and was not dependent on the factor in the conditioned medium.

Identification of the factor as activin A_2

Through successive protein fractionation steps beginning with a large quantity of the conditioned medium, we succeeded in purifying the cardiomyocyte-inducing factor as a single peak. Analysis of the amino-acid sequences of trypsinized peptide fragments using a mass spectrometer revealed that the factor was medaka activin A_2.

When the purified protein fraction was added to cultured medaka embryonic cells, it showed the same dose-dependent effects on cell growth and differentiation as the conditioned medium (Fig. 7A), and differentiated cell morphologies were indistinguishable from those formed with CM-1. Thus, the effect of myocardial cell differentiation induced by CM-1 was attributed solely to activin A_2. In addition, experiments with human activin A confirmed an effect of activin on the differentiation of cardiomyocytes (Figs. 7B, 8, 9).

Differentiation of cardiomyocytes by activin A_2

The roles of activins in mesoderm induction and axis formation during the early stages of development have been studied in amphibian embryos (Asashima, 1994; Ariizumi and Asashima, 2001; Sedohara *et al.*, 2006). Activin was found to induce a broader range of tissues, from ventral to dorsal types, in a gradient fashion depending on its concentration. For example, in the animal cap assay using *Xenopus* embryos, activin induced ventral types of mesoderm tissue at a low concentration, muscle and neural tube at a middle range of concentration, and dorsal mesoderm, such as notochord, at a high concentration (Asashima, 1994). Activin A was also shown to induce heart tissues in *Xenopus* (Ariizumi *et al.*, 2003) and newt *(Cynops pyrrhogaster)* (Asashima *et al.*, 2000) animal caps at a high concentration (10-1,000 ng/ml). In our study, it was interesting that differentiation of cardiomyocytes occurred at much lower concentrations of activin A_2 compared with those reported with amphibian embryos. In our study, the most efficient amount for the differentiation of cardiomyocytes was at 0.83 ng/ml of medaka activin A_2 or 2.5 ng/ml of human activin A.

The involvement of activins in mesoderm induction in medaka embryos was shown by Wittbrodt and Rosa (1994). They demonstrated that only maternally provided activin protein is required for the formation of mesoderm and body axis by inhibiting the

TABLE 1

PURIFICATION OF THE CARDIAC CELL INDUCING FACTOR FROM CONDITIONED MEDIUM

Steps	Total K Units	Recovery (%)	Total Protein (mg)	Specific Activity	Purification (fold)
Medium	38,500	100	72,000	0.535	1
$(NH_4)_2SO_4$	23,940	62.2	6,600	3.63	6.79
1st SP-column	22,640	58.8	139	162.9	304
Sephadex G-75	14,151	36.8	1.82	7,775	14,533
HA-column	7,640	19.8	0.41	18,634	34,830
2nd SP-column	3,080	8.0	0.011	279,859	523,101

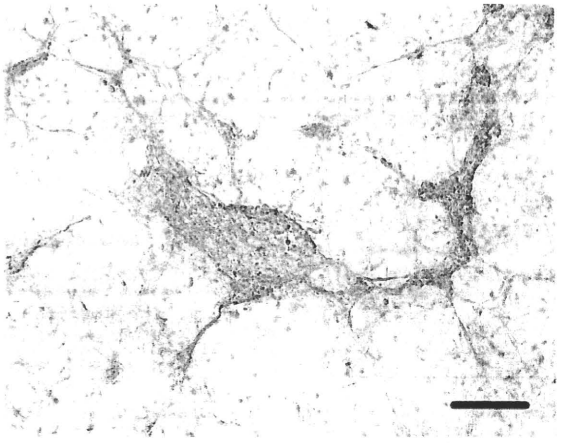

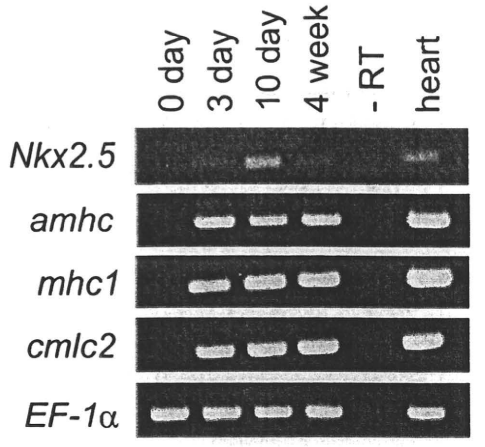

Fig. 8 (Left). Immuno-histochemical micrograph of cells incubated with human activin A for 5 days. *Bar, 100 μm.*

Fig. 9 (Right). The expression of 5 genes (*Nkx2.5, amhc, mhc1, cmlc2* and *EF-1α*) in the cells incubated with human activin A was analyzed by RT-PCR. *RNA was extracted from cells immediately after dissociation of the blastoderm (0 day), after incubation of up to 4 weeks, or from the intact medaka heart. In negative control reactions, reverse transcriptase was omitted (-RT).*

expression of zygotically transcribed activins. They also described a temporal difference in the zygotic expression of medaka activins. Activin B mRNA first appears in the late blastula, while transcripts of activin A_1 and A_2 were detected in the late gastrula. In this study, we showed that activin A_2 induces cardiomyocytes in cultured medaka embryonic cells at high frequency. We consider from our results that activin A_2 may have a specific role in the induction of heart *in vivo*. The temporal difference in the expression of activins (Wittbrodt and Rosa, 1994) may be related to functional differences in development. The possibility of a direct function of medaka activin A_2 in the differentiation of cardiomyocytes *in vivo* needs to be clarified by further investigation.

Materials and Methods

Cell culture

From the blastula-stage (stage 10-11) (Iwamatsu, 2004) medaka embryos, blastoderms were excised and were dissociated to single cells (Hyodo *et al.*, 1998). The 199ES2 medium was used for cell culture which contained 199 medium (Nissui Seiyaku Co.) supplemented with 20 mmol/L HEPES (pH 7.5), 50 nmol/L 2-mercaptoethanol, 1 mmol/L sodium pyruvate and 15% fetal calf serum (Hyclone Co.). The cell suspension was transferred to 0.1% gelatin-coated 24-well plates (Nalge Nunc Int.). Cells from 20 embryos were incubated in a well with 1.2 ml of 199ES2 medium containing a conditioned medium or a fractionated protein. The plates were incubated at 28°C.

To assay their activity during protein fractionation steps, one unit was defined as the amount of activity that induces one contracting locus in a well. Recombinant human activin A (R&D Systems, Inc.) was prepared as a 10 μg/ml stock solution according to recommendation of the supplier.

Conditioned medium

A medaka cell line (MR1) (Hyodo *et al.*, 1998) was used as feeder cell for the conditioned medium (CM-1). This fibroblastic cell line was derived from 5-day-old medaka embryos and was serially transferred in every 7-10 days for more than 5 years. To prepare CM-1, approximately $1X10^6$ cells were incubated with 5 ml of the culture medium in a culture flask ($25cm^2$, Nalge Nunc Int.). After incubation at 28°C for 5 days, the culture medium was collected and passed through a 0.2 μm membrane filter. A large scale culture was carried out in a 185 cm^2 culture flask (Nalge Nunc Int.) with 60 ml of culture medium.

Immunostaining

For immuno-histochemical study, cells dissociated from 50-60 embryos were cultured in a glass chamber slide (Nalge Nunc Int.) with 2.2 ml of 199ES2 medium containing 80 μl of CM-1. After 5 days of incubation, cells were fixed in 4% paraformaldehyde in phosphate-buffered saline (PBS) for 30 min at room temperature and rinsed with PBS. The cells were permeabilized by freezing and thawing, and incubated overnight at 4°C with an anti-troponin I antibody (monoclonal mouse anti-troponin I, bovine cardiac muscle, Advanced ImmunoChem. Inc.) at a dilution of 1:1,000. The secondary antibody was peroxidase-linked sheep anti-mouse IgG (Amersham Biosci. Co.) at a dilution of 1:100. The cells were stained in diamiobenzidine (DAB) solution (50 mM Tris-HCl, pH 7.6, 0.2 mg/ml DAB, 0.65 mg/ml NaN_3, and 0.5% H_2O_2) for 3-5 min at room temperature and then in a hematoxylin solution for 10 sec.

Electron microscope

For transmission electron microscopy, cells were fixed in 2.5% glutaraldehyde in 50 mmol/L phosphate buffer (pH 7.4) at 4°C for 1 h, postfixed in 1% OsO4 in the same buffer for 1 h, dehydrated in a graded ethanol series, and embedded in Quetol-812. Thin sections were used for staining with uranylacetate and lead solution, and then observed with an electron microscope 1200EX (JEOL Ltd).

RT-PCR

Total RNA was extracted using Trizol reagent (GIBCO) and RT-PCR was performed. At least three replicate experiments were performed for each time point. One μg of total RNA was reverse-transcribed by SuperScript II reverse-transcriptase (Invitrogen Life Technologies) using an oligo(dT) primer. RT reactions were carried out according to the manufacturer's protocol. The resulting RT reaction mixture was diluted five-fold, and 2 μl was used as template in RT-PCR reactions. PCR was performed for 35 cycles, with each cycle consisting of 94°C for 30 sec, 55°C for 40 sec and 72°C for 1 min, with additional 7 min incubation after completion of the last cycle. We used the following primers to detect these transcripts:

Nkx2.5 -forward: 5'- TTCTCTCAGGCGCAGGTGTACGAGC -3'
Nkx2.5 -reverse: 5'- GCAGGGTAGGCGTTGTA -3'

amhc -forward:	5'- ATGATGGCIGAGGAGCTGAAGAA -3'
amhc -reverse:	5'- GGTCATGATGTTCTTGTCGTAGTAG -3'
mhc1 -forward:	5'- GGAGCTGGATGATGTGGTTTC -3'
mhc1 -reverse:	5'- CATGGGCTAAGGCGTTCTTGGC -3'
cmlc2 -forward:	5'- AATGTCTTTTCCATGTTCGAAC -3'
cmlc2 -reverse:	5'- CTCCTCTTTCTCAATCACCATG -3'
EF-1α -forward:	5'- ATCGTTGCTGCTGGTGTTG -3'
EF-1α -reverse:	5'- AGGCGATGTGAGCTGTGTG -3'

Nkx2.5 is a cardiac specific homeobox gene. Atrium myosin heavy chain *(amhc)* is expressed specifically in atrium cardiomyocytes, and myosin heavy chain1 *(mhc1)* is specific for ventricle cardiomyocytes. Cardiac myosin light chain2 *(cmlc2)* is expressed in both atrium and ventricle. (Kudo, A. and Kawakami, A., personal communication). Amplification of elongation factor-1α *(EF-1α)* was used in all experiments as a positive control to ensure the quality of the mRNA.

Action potential recording

Electrophysiological studies were performed in 199 medium containing 1.8 mmol/L $CaCl_2$, 5.37 mmol/L KCl, and 25 mmol/L HEPES (pH 7.4). A Culture dish was placed on a stage of an inverted phase contrast microscope (IX-70, Olympus) at 20°C. Action potentials were recorded using a conventional glass microelectrode filled with 3 mol/L KCl and having a DC resistance of 15-30 MΩ. Intracellular recordings were made from 2-week cultured cells. Membrane potentials were measured by means of the current clamp mode (MEZ-8300, Nihon Kohden) with a built-in 4-pole Bessel filter set at 1 kHz.

Pharmacological responses

Phenylephrine (an α_1- adrenergic receptor agonist; Sigma p-6126), isoproterenol (a β_1- adrenergic receptor agonist; Sigma I-2760), clenbuterol (a β_2-adrenergic receptor agonist; Sigma C-5423) and diltiazem (a calcium channel blocker; Sigma D-2521) were used to study pharmacological responses of the spontaneously contracting cells. These reagents were dissolved in dimethyl sulfoxide at high concentrations and 1 μl solution was added to each culture medium. Final concentrations were as indicated in Fig. 5.

Purification and characterization of the protein factor

Solid ammonium sulfate was added to ten liters of CM-1 until 50% saturation was reached. The mixture was centrifuged at 13,500Xg for 20 min and the precipitate was dissolved in a 20 mmol/L Tris-HCl buffer (pH 7.5, basal buffer). The solution was extensively dialyzed against the basal buffer and then centrifuged as described above. The supernatant was applied to a SP-Sephadex column (5.6X7 cm, Amersham Bioscience Co.) previously equilibrated with the basal buffer. The column was washed with the basal buffer containing 20 mmol/L NaCl. Proteins with cardiac cell-inducing activity were eluted using the basal buffer containing 100 mmol/L NaCl. The active fractions were pooled and solid ammonium sulfate was added to 50% saturation. Then, the precipitate was collected by centrifugation, dissolved in basal buffer and applied to a Sephadex G-75 column (3.6X90 cm, Amersham Bioscience Co.) previously equilibrated with basal buffer containing 0.5 mol/L NaCl. The activity was eluted as a single peak at a position corresponding to a molecular weight of 24-28 kDa. The collected fractions were concentrated using Vivaspin 20 columns (10,000 MWCO PES, VIVASCIENCE), and applied to a hydroxylapatite column (1.0X1 cm, Bio-Gel http Gel, Bio-Lad Laboratories). The column was washed with a 50 mmol/L potassium phosphate buffer (KPB, pH 7.15) and proteins were eluted with a linear gradient of 50-150 mmol/L KPB at a flow rate of 0.5 ml/min.

The active fractions from three runs of hydroxylapatite column chromatography were collected and concentrated using Vivaspin columns. The concentrated solutions were dialyzed against basal buffer and then applied to an HPLC SP-Sepharose FF column (0.5X1 cm, Amersham Bioscience Co.), which had been equilibrated with the same buffer. After the column was washed with 10 ml of the same buffer, proteins adsorbed to the column were eluted with a linear gradient of 0-100 mmol/L NaCl in basal buffer at a flow rate of 0.5 ml/min. The proteins from the peak fraction were digested with trypsin and analysed using an Ultraflex TOF/TOF mass spectrometer (Brukar Daltonics K. K.).

Statistics

Data are expressed as mean±SE. Statistical discriminations were performed with Student's t test with $P < 0.05$ considered significant.

Acknowledgments

We thank Kamiguchi, H., Tsukamoto, H., Hasegawa, H., Kameyama, Y., Itoh, J. and Akatsuka, A., for technical assistance, Ono, M. for cell culture and RT-PCR analysis, Yamada, T., Nirasawa, T., and Kasai, S. for mass spectrometer analysis. We also thank Kubodera, S. and Nishii, Y. for helpful discussions. We are grateful to Kaji, E. H. for critically reading the manuscript. This study was supported by Grants-in-Aid from the Ministry of Education, Culture, Sports, Science and Technology, Japan (13878176 to M.H., 14657035 to M.T.).

References

ARIIZUMI, T. and ASASHIMA, M. (2001). *In vitro* induction systems for analyses of amphibian organogenesis and body patterning. *Int. J. Dev. Biol.* 45: 273-279.

ARIIZUMI, T., KINOSHITA, M., YOKOTA, C., TAKANO, K., FUKUDA, K., MORIYAMA, N., MALACINSKI, G.M. and ASASHIMA, M. (2003). Amphibian in vitro heart induction: a simple and reliable model for the study of vertebrate cardiac development. *Int. J. Dev. Biol.* 47: 405-410.

ARIIZUMI, T., KOMAZAKI, S., ASASHIMA, M. and MALACINSKI, G. M. (1996). Activin treated urodele ectoderm: a model experimental system for cardiogenesis. *Int. J. Dev. Biol.* 40: 715-718.

ASASHIMA, M. (1994). Mesoderm induction during early amphibian development. *Dev. Growth & Differ.* 36: 343-355.

ASASHIMA, M., ARIIZUMI, T. and MALACINSKI, G.M. (2000). In vitro control of organogenesis and body patterning by activin during early amphibian development. *Comp. Biochem. Physiol. B Biochem. Mol. Biol.* 126: 169-178.

BARRON, M., GAO, M. and LOUGH, J. (2000). Requirement for BMP and FGF signaling during cardiogenic induction in non-precardiac mesoderm is specific, transient, and cooperative. *Dev. Dyn.* 218: 383-393.

BRAND, T. (2003). Heart development: molecular insights into cardiac specification and early morphogenesis. *Dev. Biol.* 258: 1-19.

DENNING, C., ALLEGRUCCI, C., PRIDDLE, H., BARBADILLO-MUNOZ, M. D. ANDERSON, D., SELF, T., SMITH, N. M., PARKIN, C. T. and YOUNG, L. E. (2006). Common culture conditions for maintenance and cardiomyocyte differentiation of the human embryonic stem cell lines, BG01 and HUES-7. *Int. J. Dev. Biol.* 50: 27-37.

FAN, L. and COLLODI, P. (2006). Zebrafish embryonic stem cells. *Methods Enzymol.* 418: 64-77.

FUKUDA, K. and YUASA, S. (2006). Stem cells as a source of regenerative cardiomyocytes. *Circ Res.* 98: 1002-1013.

HONG, Y., WINKLER, C. M. and SCHARTL, M. (1998). Efficiency of cell culture derivation from blastula embryos and of chimera formation in the medaka *(Oryzias latipes)* depends on donor genotype and passage number. *Dev. Genes. Evol.* 0208: 595-602.

HYODO, M., KATSUMATA, M., TAKAGI, S., TAKADA, T., MIYAJIMA, S., MOROZUMI, T. and MATSUHASHI, M. (1998). Characterization of developmental potential in isolated medaka blastomeres and cultured embryonic cells. *J. Mar. Biotechnol.* 6: 23-29.

IWAMATSU, T. (2004). Stages of normal development in the medaka *Oryzias latipes*. *Mech. Dev.* 121: 605-618.

KASAHARA, M., NARUSE, K., SASAKI, S., NAKATANI, Y., QU, W., AHSAN, B., YAMADA, T., NAGAYASU, Y., DOI, K., KASAI, Y., JINDO, T., KOBAYASHI, D., SHIMADA, A., TOYODA, A., KUROKI, Y., FUJIYAMA, A., SASAKI, T., SHIMIZU, A., ASAKAWA, S., SHIMIZU, N., HASHIMOTO, S., YANG, J., LEE, Y., MATSUSHIMA, K., SUGANO, S., SAKAIZUMI, M., NARITA, T., OHISHI, K.,

HAGA, S., OHTA, F., NOMOTO, H., NOGATA, K., MORISHITA, T., ENDO, T., SHIN-I, T., TAKEDA, H., MORISHITA, S. and KOHARA, Y. (2007). The medaka draft genome and insights into vertebrate genome evolution. *Nature* 447: 714-719.

KEHAT, I., KENYAGIN-KARSENTI, D., SNIR, M., SEGEV, H., AMIT, M., GEPSTEIN, A., LIVNE, E., BINAH, O., ITSKOVITZ-ELDOR, J. and GEPSTEIN, L. (2001). Human embryonic stem cells can differentiate into myocytes with structural and functional properties of cardiomyocytes. *J. Clin. Invest.* 108: 407-414.

LADD, A.N., YATSKIEVYCH, T.A. and ANTIN, P.B. (1998). Regulation of avian cardiac myogenesis by activin/Tgfβ and bone morphogenetic proteins. *Dev. Biol.* 204: 407-419.

LAFLAMME, M.A., CHEN, K.Y., NAUMOVA, A.V., MUSKHELI, V., FUGATE, J.A., DUPRAS, S.K., REINECKE, H., XU, C., HASSANIPOUR, M., POLICE, S., O'SULLIVAN, C., COLLINS, L., CHEN, Y., MINAMI, E., GILL, E.A., UENO, S., YUAN, C., GOLD, J. and MURRY, C.E. (2007). Cardiomyocytes derived from human embryonic stem cells in pro-survival factors enhance function of infarcted rat hearts. *Nature Biotechnol.* 25: 1015-1024.

LOUGH, J., BARRON, M., BROGLEY, M., SUGI, Y., BOLENDER, D.L. and ZHU, X. (1996). Combined BMP-2 and FGF-4, but neither factor alone, induces cardiogenesis in non-precardiac embryonic mesoderm. *Dev. Biol.* 178: 198-202.

LOUGH, J. and SUGI, Y. (2000). Endoderm and Heart Development. *Dev. Dyn.* 217: 327-342.

PASSIER, R., OOSTWAARD, D.W., SNAPPER, J., KLOOTS, J., HASSINK, R.J., KUIJK, E., ROELEN, B., DE LA RIVIERE, A.B. and MUMMERY, C. (2005). Increased cardiomyocyte differentiation from human embryonic stem cells in serum-free cultures. *Stem Cells* 23: 772-780.

SCHULTHEISS, T.M., XYDAS, S. and LASSAR, A.B. (1995). Induction of avian cardiac myogenesis by anterior endoderm. *Development* 121: 4203-4214.

SEDOHARA, A., SUZAWA, K. and ASASHIMA, M. (2006). Comparison of Induction during development between Xenopus tropicalis and Xenopus laevis. *Int. J. Dev. Biol.* 50: 385-392.

SUGI, Y. and LOUGH, J. (1995). Activin-A and FGF-2 mimic the inductive effects of anterior endoderm on terminal cardiac myogenesis in vitro. *Dev. Biol.* 168: 567-574.

TADA, T., HIRONO, I., AOKI, T. and TAKASHIMA, F. (1998). Cloning and sequencing of carp and medaka activin subunit genes. *Fish Sci.* 64: 680-685.

TAKAHASHI, K., TANABE, K., OHNUKI, M., NARITA, M., ICHISAKA, T., TOMODA, K. and YAMANAKA, S. (2007). Induction of pluripotent stem cells from adult human fibroblasts by defined factors. *Cell* 131: 861-872.

TAKAHASHI, K. and YAMANAKA, S. (2006). Induction of pluripotent stem cells from mouse embryonic and adult fibroblast cultures by defined factors. *Cell* 126: 663-676.

THOMSON, J.A., ITSKOVITZ-ELDOR, J., SHAPIRO, S.S., WAKNITZ, M.A., SWIERGIEL, J.J., MARSHALL, V.S. and JONES, J.M. (1998). Embryonic stem cell lines derived from human blastocysts. *Science* 282: 1145-1147.

VAN LAAKEA, L.W., PASSIER, R., MONSHOUWER-KLOOTS, J., VERKLEIJ, A.J., LIPS, D.J., FREUND, C., DEN OUDEN, K., WARD-VAN OOSTWAARD, D., KORVING, J., TERTOOLEN, L.G., VAN ECHTELD, C.J., DOEVENDANS, P.A. and MUMMERY, C.L. (2007). Human embryonic stem cell-derived cardiomyocytes survive and mature in the mouse heart and transiently improve function after myocardial infarction. *Stem Cell Res.* 1: 9-24.

WITTBRODT, J. and ROSA, F.M. (1994). Disruption of mesoderm and axis formation in fish by ectopic expression of activin variants: the role of maternal activin. *Genes & Dev.* 8: 1448-1462.

XU, C., POLICE, S., RAO, N., and CARPENTER, M.K. (2002). Characterization and enrichment of cardiomyocytes derived from human embryonic stem cells. *Circ. Res.* 91: 501-508.

YATSKIEVYCH, T.A., LADD, A.N. and ANTIN, P.B. (1997). Induction of cardiac myogenesis in avian pregastrula epiblast: the role of the hypoblast and activin. *Development* 124: 2561-2570.

YUTZEY, K.E. and KIRBY, M.L. (2002). Wherefore heart thou? Embryonic origins of cardiogenic mesoderm. *Dev. Dyn.* 223: 307-320.

ZAFFRAN, S. and FRASCH, M. (2002). Early signals in cardiac development. *Circ. Res.* 91: 457-469.

Am J Physiol Endocrinol Metab 296: E1363–E1373, 2009.
First published March 17, 2009; doi:10.1152/ajpendo.90767.2008.

Ligand-based gene expression profiling reveals novel roles of glucocorticoid receptor in cardiac metabolism

Noritada Yoshikawa,[1,2]* Masao Nagasaki,[3]* Motoaki Sano,[4,6] Satori Tokudome,[4] Kazuko Ueno,[3] Noriaki Shimizu,[1] Seiya Imoto,[3] Satoru Miyano,[3] Makoto Suematsu,[5] Keiichi Fukuda,[4] Chikao Morimoto,[1,2] and Hirotoshi Tanaka[1,2]

[1]Division of Clinical Immunology, Advanced Clinical Research Center, [2]Research Hospital, [3]Laboratory of DNA Information Analysis, Human Genome Center, Institute of Medical Science, University of Tokyo, Tokyo; [4]Department of Regenerative Medicine and Advanced Cardiac Therapeutics, [5]Department of Biochemistry and Integrative Medical Biology, Keio University School of Medicine, Tokyo; and [6]Precursory Research for Embryonic Science and Technology, Japan Science and Technology Agency, Saitama, Japan

Submitted 16 September 2008; accepted in final form 13 March 2009

Yoshikawa N, Nagasaki M, Sano M, Tokudome S, Ueno K, Shimizu N, Imoto S, Miyano S, Suematsu M, Fukuda K, Morimoto C, Tanaka H. Ligand-based gene expression profiling reveals novel roles of glucocorticoid receptor in cardiac metabolism. *Am J Physiol Endocrinol Metab* 296: E1363–E1373, 2009. First published March 17, 2009; doi:10.1152/ajpendo.90767.2008.—Recent studies have documented various roles of adrenal corticosteroid signaling in cardiac physiology and pathophysiology. It is known that glucocorticoids and aldosterone are able to bind glucocorticoid receptor (GR) and mineralocorticoid receptor, and these ligand-receptor interactions are redundant. It, therefore, has been impossible to delineate how these nuclear receptors couple with corticosteroid ligands and differentially regulate gene expression for operation of their distinct functions in the heart. Here, to particularly define the role of GR in cardiac muscle cells, we applied a ligand-based approach involving the GR-specific agonist cortivazol (CVZ) and the GR antagonist RU-486 and performed microarray analysis using rat neonatal cardiomyocytes. We indicated that glucocorticoids appear to be a major determinant of GR-mediated gene expression when compared with aldosterone. Moreover, expression profiles of these genes highlighted numerous roles of glucocorticoids in various aspects of cardiac physiology. At first, we identified that glucocorticoids, via GR, induce mRNA and protein expression of a transcription factor Kruppel-like factor 15 and its downstream target genes, including branched-chain aminotransferase 2, a key enzyme for amino acid catabolism in the muscle. CVZ treatment or overexpression of KLF15 decreased cellular branched-chain amino acid concentrations and introduction of small-interfering RNA against KLF15 cancelled these CVZ actions in cardiomyocytes. Second, glucocorticoid-GR signaling promoted gene expression of the enzymes involved in the prostaglandin biosynthesis, including cyclooxygenase-2 and phospholipase A2 in cardiomyocytes. Together, we may conclude that GR signaling should have distinct roles for maintenance of cardiac function, for example, in amino acid catabolism and prostaglandin biosynthesis in the heart.

endocrinology; cardiovascular system; KLF15; cylooxygenase-2; phospholipase A2

GLUCOCORTICOID HORMONES ARE essential for homeostatic regulation and physiological maintenance of a variety of organ functions. Concerning the heart, numerous observations have suggested that glucocorticoids as well as aldosterone (ALD) have been shown to exert direct effects on cardiomyocytes and help maintain various cardiac functions. For example, it is shown that a synthetic glucocorticoid, dexamethasone (DEX), significantly increases the L-type Ca^{2+} currents (51) and inhibits inducible nitric oxide synthase activity in rat cardiomyocytes (42). Moreover, DEX treatment enhances the development of contractile tension and increases contraction and relaxation velocities in cardiac muscle (35). The decrease in contractile force of rat papillary muscle induced by adrenalectomy is prevented by DEX treatment (27) by modulating membrane Ca^{2+} transport and K^+ channels (33, 35, 50, 51). Short-term treatment with DEX has been shown to decrease resting heart rate in healthy human volunteers (5). It, thus, is apparent that glucocorticoids play essential roles in regulation of cardiac electrical and mechanical activities. On the other hand, numerous studies have documented the pathological consequences and deleterious effects of abnormal or excessive glucocorticoid signalings. Not only hypercortisolemia in patients with Cushing's syndrome but also the chronic therapeutic use of glucocorticoids is associated with several side effects, including adverse cardiovascular events, such as hypertension and left ventricular hypertrophy (48). Glucocorticoid excess also induces metabolic syndrome with hyperglycemia, dyslipidemia, and obesity, which is associated with early and progressive atherosclerosis, contributing to a cluster of cardiovascular risk factors, including heart failure (48). Moreover, several clinical studies have documented the distinct role of glucocorticoids in the prognosis of cardiac diseases; for example, rheumatoid factor-positive but not negative patients with rheumatoid arthritis were at increased risk of cardiovascular events following exposure to glucocorticoids (8), and, in patients with chronic heart failure, higher serum levels of cortisol and ALD were independent predictors of increased mortality risk (16).

Glucocorticoids and mineralocorticoids bind to the nuclear receptors glucocorticoid receptor (GR) and mineralocorticoid receptor (MR), both of which are transcription factors and expressed in cardiomyocytes. However, the role of these receptors in cardiac physiology remains elusive. Indeed, the ligand-receptor interactions are complicated, as both ALD and glucocorticoids can activate cardiac MR, thereby directly affecting heart function (48). Some of the cardiac or peripheral effects of glucocorticoids may be mediated at least in part by MR activation. In "classical" ALD target cells (i.e., kidney and colon), MR is protected from illicit occupation by glucocorti-

* N. Yoshikawa and M. Nagasaki contributed equally to this work.

Address for reprint requests and other correspondence: H. Tanaka, Division of Clinical Immunology, Advanced Clinical Research Center, Institute of Medical Science, Univ. of Tokyo, 4-6-1, Shirokanedai, Minato-ku, Tokyo 108-8639, Japan (e-mail: hirotnk@ims.u-tokyo.ac.jp).

coids because of the presence of 11β-hydroxysteroid dehydrogenase type II (11βHSD2), an enzyme that converts cortisol (human)/corticosterone (COR, rodents) into inactive metabolites. Cardiomyocytes belong to the so-called "nonclassical" ALD target tissues that express both GR and MR, but not 11βHSD2. In cardiomyocytes, thus, MR is not protected from occupancy by glucocorticoids and is not ALD selective. Taking into account that circulating cortisol/COR levels are at least 100-fold higher than those of ALD, and that MR has the same affinity for ALD and glucocorticoids, MR, as well as GR, may be permanently occupied by glucocorticoids, and glucocorticoid effects could be mediated by both GR and MR (48). The recent advent of microarray and other technologies has facilitated the identification of a number of glucocorticoid-regulated genes (1, 20, 34, 36, 45), and it becomes apparent that the profile of those glucocorticoid-target genes differs according to the cell types and the mode of interaction with ligands (49). However, because of the redundancy of the ligand-receptor interaction, not a single study could clearly differentiate target genes for cardiac GR and MR. Recently, a transgenic mouse model with conditionally inducible cardiac-specific expression of human GR was generated to preclude secondary effects due to general glucocorticoid-induced alterations and to investigate the specific role of GR in cardiomyocytes, and electrophysiological phenotyping indicated that cardiac GR overexpression resulted in conduction defects, with high-degree atrio-ventricular block (39). These results strongly support such an idea that GR has as yet unknown but essential roles in the heart. It, therefore, is important to delineate how these nuclear receptors, especially GR, differentially couple with ligands and regulate gene expression for operation of their distinct functions in cardiomyocytes.

We previously reported that a synthetic glucocorticoid, cortivazol (CVZ), could be extremely specific for GR and does not crossreact with MR (52, 53). Given this, we indicated that a ligand-based approach involving CVZ and GR antagonist RU-486 might be applied to define the role of GR in nonclassical ALD target tissues. In the present study, we performed microarray analysis based on this ligand-based approach and differentially characterized corticosteroid target genes, and the distinct role of GR in cardiomyocytes was discussed.

MATERIALS AND METHODS

Reagents and antibodies. CVZ was kindly gifted from Sanofi-Aventis (Paris, France). COR, ALD, interleukin (IL)-1β, lipopolysaccharide, estradiol, progesterone, and RU-486 were purchased from Sigma (St. Louis, MO). MG-132 was purchased from Calbiochem (San Diego, CA). Other reagents were from Nacalai Tesque (Kyoto, Japan) unless otherwise specified. Anti-GR (sc-1004), anti-cyclooxygenase-2 (COX-2, sc-1747), and anti-KLF15 (sc-34827) antibodies were obtained from Santa Cruz Biotechnology (Santa Cruz, CA). Anti-α-actinin (A7811) and anti-FLAG (F1804) antibodies were obtained from Sigma.

Plasmids, small-interfering RNA oligonucleotides, and recombinant adenoviruses. To construct the expression plasmids for FLAG-tagged rat GR and MR, either full-length cDNAs for rat GR or MR were inserted in p3xFLAG-CMV10 vector (Sigma). The glucocorticoid response element (GRE)-driven reporter plasmid p2xGRE-LUC was described previously (52). Small-interfering RNA (siRNA) oligonucleotides against rat GR (Silencer Predesigned siRNA ID: 199951) and control siRNA (Silencer Negative control siRNA no. 1: 07606954A) were purchased from Ambion (Austin, TX). siRNA oligonucleotides against rat KLF15 (Stealth Select RNAi RSS340443) were purchased from Invitrogen (Carlsbad, CA). Recombinant adenoviruses encoding FLAG-tagged rat KLF15 and Cre-recombinase were generated by using the Adenovirus Cre/loxP-regulated Expression Vector Set (TaKaRa, Otsu, Japan) as per the manufacturer's instructions and as previously described (44). Recombinant adenoviruses prepared from 293 cells were purified with Virakit AdenoMini-24 (Virapur, San Diego, CA) and titrated using an Adeno-X Rapid Titer Kit (TaKaRa).

Cell culture. COS-7 cells were obtained from RIKEN Cell Bank (Tsukuba, Japan) and cultured in DMEM (Invitrogen) supplemented with 10% FCS (Sigma-Aldrich, St. Louis, MO) and antibiotics in a humidified atmosphere at 37°C with 5% CO_2. Primary cultures of cardiomyocytes were prepared as described previously (40). In brief, the ventricles of 1-day-old neonatal Wistar rats (CLEA Japan, Tokyo, Japan) were dissociated in 0.03% trypsin, 0.03% collagenase, and 20 μg/ml of DNase I. The cardiomyocytes and cardiac fibroblasts were separately prepared on the basis of their differential adhesiveness. Attached cells (mostly cardiac fibroblasts) were subcultured two times to deplete cardiomyocytes, and the third passage cells were used. Cardiomyocytes were seeded at a density of 1×10^5 cells/cm^2 on gelatin-coated dishes and grown in medium 199/DMEM (Invitrogen) supplemented with 10% FCS and antibiotics in a humidified atmosphere at 37°C with 5% CO_2. Concerning animal experiments, all procedures and protocols were approved by the Animal Care and Use Committee of Keio University.

Immunofluorescence. FLAG-tagged rat GR- or MR-expressing COS-7 cells were plated on glass coverslips in a six-well plate. Fixed and permeabilized cells were blocked with blocking buffer (3% BSA and 0.1% Triton X in Tris-buffered saline). The cells were then stained with primary antibodies against FLAG (1:500) for 1 h at room temperature, and then, secondary antibodies conjugated with Alexa Fluor 488 (1:500, Invitrogen) were applied for 1 h at room temperature. The stained cells were observed by confocal laser scanning microscopy (LSM510; Carl Zeiss, Jena, Germany) with appropriate emission filters.

Western blotting. Whole cell extracts were prepared in Nonidet P-40 (NP-40) lysis buffer (150 mM NaCl, 1.0% NP-40, 50 mM Tris, pH 8.0, and protease inhibitor cocktail) and boiled in SDS sample buffer, analyzed by SDS-PAGE, and electrically transferred to a polyvinyl difluoride membrane (Millipore, Bedford, MA). Subsequently, immunoblotting was performed with anti-GR, anti-α-actinin, anti-KLF15, anti-FLAG, or anti-COX-2 antibodies diluted at 1:1,000, followed by horseradish peroxidase-conjugated secondary antibodies (Amersham Biosciences, Buckinghamshire, UK) diluted at 1:2,000. Antibody-protein complexes were visualized using the enhanced chemiluminescence method according to the manufacturer's protocol (Amersham Biosciences). Signal intensity of the band for GR relative to that for α-actinin was quantified using the analysis software from the National Institutes of Health (NIH image 1.62).

Transfection and reporter gene assay. Transient transfection and reporter gene assay were performed as described previously (53). In brief, cells were plated on 6-cm-diameter culture dishes, and cell culture medium was replaced with serum-free medium OPTI-MEM lacking phenol red (Invitrogen) before transfection. Plasmids or siRNA oligonucleotides were mixed with Lipofectamine 2000 transfection reagent (Invitrogen) and added to the culture according to the manufacturer's protocol. The total amount of the plasmids was kept constant by adding an irrelevant plasmid (pGEM3Z was used unless otherwise specified). After 6 h of incubation, the medium was replaced with fresh OPTI-MEM, and the cells were further cultured in the presence or absence of various reagents for 24 h at 37°C. In reporter gene assay, whole cell extracts were prepared in Cell Culture Lysis Reagent (Promega, Madison, WI) on ice for 15 min followed by centrifugation for 20 min at 20,000 *g*. Luciferase enzyme activity was determined using the Luciferase Assay System (Promega) and a luminometer (Promega) according to the manufacturer's protocol.